Swiss Journal of Palaeontology

RESEARCH

Open Access

Cranial osteology of *Cynodictis* (Amphicyonidae), the oldest European carnivoran

Kévin Le Verger[1,2*], Charlène Letenneur[2], Valentin Fischer[3], Marcelo R. Sánchez-Villagra[1], Sandrine Ladevèze[2] and Floréal Solé[4]

Abstract

The amphicyonids, colloquially called 'beardogs', are one of the oldest known groups of caniformians, taking part in the initial radiation of this carnivoran clade. While the oldest American occurrences from the Middle Eocene have been investigated in detail, the European material remains understudied. The oldest European occurrences suggest an appearance of caniformians in the Priabonian of southern France and a diversification during the Oligocene, after a major faunal turnover following drastic climatic and environmental changes, the '*Grande Coupure*'. Their first representative is the amphicyonid *Cynodictis lacustris*, the cranial osteology of which is of much relevance for the systematics of Caniformia. A well-preserved cranium of *Cynodictis lacustris* was collected in the Phosphorites of Quercy (Lot, France) in the late 1960s. The exceptional preservation of the specimen allows us to describe the osteology, make substantial comparative observations and propose biological interpretations, leading to a partial reconstruction of the cranial vascularization, innervation, and musculature. We also reconstruct the ecological evolution of the European amphicyonids from the Paleogene based on their body masses and diets, leading to identify three different faunas: (1) the oldest one (Priabonian) is characterized by body mass around 10 kg, well-exemplified by *Cynodictis lacustris*; (2) the second (Rupelian) groups taxa from 30 to 50 kg; (3) the last one (Chattian) differs from the two others by the presence of large amphicyonids (ca. 140 kg) and the low number of hypercarnivorous amphicyonids. The in-depth investigation of this exceptional specimen provides new material for the systematic and paleoecological understanding of Paleogene amphicyonids.

Keywords Carnivora, *Cynodictis*, Cranium, Innervation, Vascularization, Paleoecology

Introduction

Many localities in Europe show high species richnesses in mammals during the Paleogene (Biochrom'97 1997). One of the main climatic events, the Eocene–Oligocene cooling (ca. 33.9 Mya), was a global shift from greenhouse to icehouse climate, concurrent with a major faunal upheaval for a large part of the mammalian clades present in Europe at that time (e.g., Legendre et al., 1991; Weppe et al., 2023). This event, called the '*Grande Coupure*', signals environmental changes of great magnitude characterized by an increased aridity and the development of open habitats such as savannahs or steppes at the expense of closed habitats such as forests (Legendre,

Handling editor: Thomas Martin

†Sandrine Ladevèze And Floréal Solé are Co-last authors.

*Correspondence:
Kévin Le Verger
kevin.leverger@pim.uzh.ch
[1] Department of Paleontology, University of Zurich, Karl-Schmid-Strasse 4, 8006 Zurich, Switzerland
[2] Museum National d'Histoire Naturelle, Centre de Recherche en Paléontologie – Paris, UMR 7207 CR2P MNHN/CNRS/UPMC, Sorbonne Université, 8 Rue Buffon, CP 38, 75005 Paris, France
[3] Evolution & Diversity Dynamics Lab, UR Geology, Université de Liège, Allée du 6 Août 14, 4000 Liège, Belgium
[4] Directorate Earth and History of Life, Royal Belgian Institute of Natural Sciences, Rue Vautier 29, 1000 Brussels, Belgium

1987; Legendre & Hartenberger, 1992). These environmental modifications are the main cause of the extinction of endemic species, as first noted by Stelhin (1909), and also drove a massive immigration from Asia (Legendre & Hartenberger, 1992), as recently emphasized in artiodactyls (Weppe et al., 2023). This faunal turnover occurred between MP20 and MP21 reference levels (Legendre et al., 1991), and more precisely between 34.1 and 33.55 Mya, according to Weppe et al. (2023)

At the core of the trophic interactions induced by this great mammalian diversification, two clades of predatory mammals stand out: Hyaenodonta and Carnivoramorpha (Solé et al., 2011, 2014, 2016, 2022a). These carnivorous mammals represent an informative example of the faunal disruption characteristic of the '*Grande Coupure*'. Hyaenodonts are abundant and much more diverse in the Eocene (56 Ma to 33.9 Ma) than carnivoramorphans, whereas the crown clade Carnivora (Wesley-Hunt & Flynn, 2005), dominate considerably from the Oligocene onwards (33.9 Ma to 23.03 Ma) (Solé et al., 2022a). While the vast majority of carnivorans appear and diversify during the Oligocene, only one clade originates and shows diversity during the Eocene in Europe: Amphicyonidae.

Amphicyonidae or "bear-dogs"—so colloquially called because of their anatomical resemblances with both canids and ursids—are dated, for the oldest occurrences, from the Bartonian (Duchesnean North American Land Mammal 'age') of North America (Tomiya & Tseng, 2016). With more than 34 genera (Mckenna & Bell, 1997), and a stratigraphic distribution ranging from the Middle Eocene to the Late Miocene (Goswami & Friscia, 2010), the phylogenetic position of amphicyonids is much unresolved (Viranta, 1996). Initially considered as closely related to Canidae (Matthew & Granger, 1924; Petter, 1966; with a relatively recent revival of this hypothesis Spaulding & Flynn, 2012), they later have been regarded as the sister group of Ursidae (Ginsburg, 1966; Hough, 1948; Hunt, 1977; Wyss & Flynn, 1993) or the sister group of Arctoidea (a group formed by ursids, pinnipeds and musteloids; Finarelli, 2008; Hunt, 1996, 1998). Finally, the most recent studies find the bear-dogs as the sister group to all caniformians (Tomiya & Tseng, 2016; Tomiya et al., 2021; Wesley-Hunt & Flynn, 2005). However, this last hypothesis remains fragile (e.g., Wang et al., 2022; Zhang et al., 2023) as the amphicyonids included in these studies correspond only to North American taxa, with the exception of one European taxon, *Cynodictis*. Although incongruence characterizes the compilation of phylogenetic hypotheses for Amphicyonidae, a general consensus holds that this group is close to the origin of Caniformia and the crown Carnivora. In this regard, *Cynodictis* is always recovered as the sister group to all other amphicyonids, even though this genus enters the fossil record more recently (i.e., Priabonian) while its morphology is similar to that of early North American Bartonian caniforms such as *Lycophocyon* (Tomiya, 2011), a typical case of ghost lineage. It is thus crucial to overcome the severe lack of data for the Paleogene European amphicyonids, in order to better understand the early diversification of Carnivora.

In Europe, the genus *Cynodictis* is known from the Priabonian (MP 18), which makes it the oldest occurrence of Amphicyonidae (and consequently of Carnivora; Bonis, 1978; Kotsakis, 1980). *Cynodictis* is also known to retain plesiomorphic characters within Amphicyonidae (Tomiya & Tseng, 2016), but this genus is only known by fragmentary data, mostly dental remains. *Cynodictis* and other European amphicyonids have been documented so far by a few relatively fragmentary cranial remains (Le Verger et al., 2020). As indicated by Tomiya and Tseng (2016), no synthesis of European Amphicyonidae has been made so far and only a study of *Cynodictis* in relation to other genera, can shed light on our knowledge of the history of Amphicyonidae, and, by extension, of early carnivorans. This is what we aim for, by studying new cranial material of *Cynodictis*.

From 1967 to 1970, in France, the palaeontologist Dr. B. Lange-Badré led the excavation of a cavity named Aubrelong 3 belonging to the gigantic karst formation Phosphorites of Quercy (Gèze, 1974); this locality was reassigned to Aubrelong 1 (Dr. M. Vianey-Liaud, personal communication) and dated from the earliest Oligocene (MP 21), close to Eocene–Oligocene transition. The team she led uncovered several specimens in a beautiful state of preservation but had never been studied. Among them were two almost complete carnivoran crania of exceptional preservation quality. Informally, the first was identified as belonging to the genus *Amphicynodon gracilis*, one of the oldest known genera related to ursids, while the second was attributed to an amphicyonid: *Cynodictis lacustris*.

Given the completeness of the material and the highly fragmentary state of the anatomical data available for Amphicyonidae, our main objective is to present a detailed and comparative anatomical description of *Cynodictis lacustris*. This cranium is here compared not only to those of other available species of Amphicyonidae from the Paleogene of Europe, including other known remains of *Cynodictis*, but also to those of other carnivorans from the Oligocene. Our description aims at providing a maximum of information concerning the cranial anatomy of this genus while proposing several biological interpretations and discussing the main features of *Cynodictis* with respect to the other carnivorans. Moreover, in order to situate *Cynodictis lacustris* among the history of the amphicyonids, notably in the critical context that represents the Eocene–Oligocene boundary

in Europe, we here propose an analysis of the ecological evolution of amphicyonids from the Paleogene of Europe through their body mass, as was done for the Miocene amphicyonids by Viranta (1996) and Solé et al. (2022b). Such analysis is supported by the relatively complete nature of the European fossil record and the taxonomic and ecological diversity of amphicyonids, enabling to address future comparisons of amphicyonid evolution worldwide and the success of Caniformia.

Materials and methods

Geological setting

Discovered in 1869 by mining, the many deposits belonging to a gigantic karst system are pockets filled with extremely fossiliferous phosphates: the Phosphorites of Quercy (Cavaillé, 1974). These paleokarst faunas range from the early Eocene to the early Miocene (Escarguel et al., 2008; Legendre et al., 1992; Maitre et al., 2006, 2008; Maitre, 2014; Renaud et al., 1978; Rémy et al., 1987; Sigé et al., 1991). Such expanded temporal record and abundant fossil record makes the Quercy a key area for understanding the evolution of the European Paleogene mammals (Escarguel et al., 2008; Legendre & Hartenberger, 1992; Rémy et al., 1987). Here we study a new, almost complete cranium of *Cynodictis lacustris* (MNHN.F.Qu 17762), which was extracted from a deposit dated as early Rupelian, just younger than the Eocene–Oligocene transition (MP 21). Whereas considered first to belong to the Aubrelong 3 locality (Gèze, 1974), it may well be a continuation of the Aubrelong 1 locality (Dr. M. Vianey-Liaud, personal communication), a hypothesis that we follow here. Between 1967 and 1970, Dr. B. Lange-Badré (CNRS) conducted the excavation of this cavity composed of two main levels of clay including calcites and phosphorites over approximately six meters (Fig. 1, Gèze, 1974). Several specimens were discovered in an excellent state of preservation and were stored in Lange-Badré's personal collections. At her death, her collections were transferred to the Museum national d'Histoire naturelle at Paris, where they were rediscovered and for which we can now provide comprehensive descriptions.

Comparative anatomy

Sampling

Amphicyonidae are taxonomically diverse, although many species in this clade have been described on the bases of highly fragmented specimens, possibly causing an overestimation of the specific diversity of the clade. *Cynodictis* is an evident example, with over 20 described species and only six or seven currently valid (Kotsakis, 1980; Le Verger et al., 2020). Facing the incompleteness of cranial remains of European Paleogene amphicyonids (as compared to dental remains, Le Verger et al., 2020), we decided to compare MNHN.F.Qu 17762 to a maximum of taxa within the carnivoraforms, restricted chronologically to the Paleogene and spatially to Europe. Our sample thus includes ten species among which are nine crania of amphicyonids, two crania of ursids, two crania of feliforms, and two crania of non-carnivoran carnivoramorphans (Table 1). All specimens come from French deposits: eleven from the Phosphorites of Quercy and four from the Allier Basin. The specimens were observed with the natural eye and with a Nikon SMZ1000 binocular loupe. Measurements (Table 2) were taken with a pair of callipers to the nearest 0.01 mm.

Anatomical nomenclature

The comparative anatomical description of the cranium of *Cynodictis lacustris* is a large expansion of the brief descriptions provided by Carlsson (1914), Teilhard de Chardin (1915) and Petter (1966), part of which was produced for describing *C. intermedius* Filhol, 1876, a species now synonymized with *Cynodictis lacustris* (Kotsakis, 1980). The taxonomy of *Cynodictis* follows our previous work (Le Verger et al., 2020), and the cranial nomenclature presented by Wible and Spaulding (2013) for *Nandinia binotata* Gray, 1830, the African palm civet. Biological interpretations of foramina, grooves, processes, crests, bulges, and cavities refer mostly to our knowledge of the soft anatomy of *Canis familiaris* Linnaeus, 1758 (Evans, 1993). The nomenclature for the molariform dentition follows Szalay (1969) and that for premolars Ginsburg (1999).

Comparative ecology

Paleogene amphicyonids sampling

Our study on the evolution of the European amphicyonids is based on a sample including 27 species within 14 genera. We include all amphicyonids known in Europe from the Eocene and Oligocene for which we have information on the lower dentition, at least the m1, based on the literature (*e.g.*, Springhorn, 1977; Kotsakis, 1980; Bonis, 2020) and the species described herein. When possible (16 taxa), the amphicyonids were assigned to an MP according to BiochroM'97 (1997) and recent data from the literature (Table S1).

Body mass

We estimated the body mass (BM, in kg) from dental remains, using the equation established by Van Valkenburgh (1990) for a set of carnivorans and dasyuromorphians: $\text{Log10(BM)} = [2{,}97 \times \text{Log10(Lm1)}] - 2{,}27$; where Lm1 is the length of the first lower molar in mm. We estimated BM for 27 amphicyonid species (Table S1). For comparison purposes, we also estimated the BM of

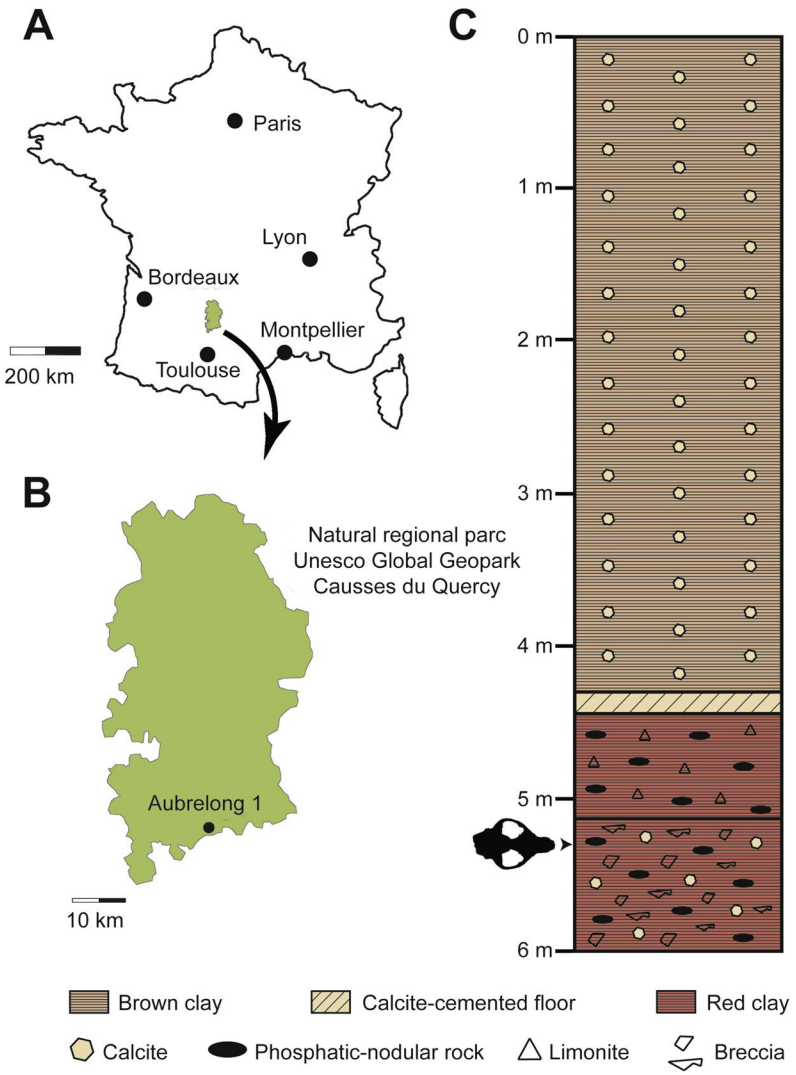

Fig. 1 Aubrelong deposit 1. **A**, location of most of the Quercy phosphorites. **B**, location of the Aubrelong commune. **C**, Stratigraphic profile of Aubrelong 1 (~6 m) following Gèze (1974). All the fossils collected during the excavation by Dr. B. Lange-Badré, including *Cynodictis lacustris* MNHN.F.Qu 17762, come from the brecciated level (~5.15 m)

six amphicynodontids and one ursid from the MP22 of Europe (Table S1).

Diet

Diet was inferred from the indices and categories defined by Van Valkenburg (1988, 2007) for Carnivora. We used four categories: (1) Hypercarnivore, the organism feeds on more than 70% meat; (2) Scavenger, the organism feeds on more than 70% meat and large bones; (3) Mesocarnivore, the organism feeds on 50% to 70% fruit and/or insects; (4) Hypocarnivore, the organism feeds on less than 50% meat, fruit and/or insects. Van Valkenburg (1988) proposed five indices for inferring the diet of a carnivoran. In our study, the two most representative were selected: the Relative Blade Length (RBL) index (ratio of the length of the m1 trigonid to the total length of the m1) and the Relative Premolar Size (RPS) index (ratio of the width of the largest premolar to the square root of the weight). These indices are compared with characteristic values for each category to infer a diet for the 27 amphicyonids in our sample. The diet of two species has not been determined due to lack of data (see Results).

Institutional abbreviations

FSL, Faculté des Sciences de Lyon; LA, Langy; MHNG, Muséum d'Histoire Naturelle de Genève; MNHN.F, fossil collection of the Muséum National d'Histoire Naturelle, Paris, France; Qu, fossil collection from the Phosphorites

Table 1 Sample list including the comparative sample

Family	Species	Material	Locality—age
Stem-Carnivora	*Paramiacis exilis* Mathis, 1985	Subcomplete Cranium MNHN.F.Qu 8752	Phosphorites of Quercy Late Eocene/Early Oligocene
Stem-Carnivora	*Quercygale angustidens* Filhol, 1872	Subcomplete Cranium MNHN.F.Qu 8755	Phosphorites of Quercy Late Eocene/Early Oligocene
Stenoplesictidae	*Palaeoprionodon lamandini* Filhol, 1880	Subcomplete Cranium MNHN.F.Qu 9348	Phosphorites of Quercy Late Eocene/Early Oligocene
Stenoplesictidae	*Palaeoprionodon lamandini* Filhol, 1880	Subcomplete Cranium MNHN.F.Qu 9371	Phosphorites of Quercy Late Eocene/Early Oligocene
Amphicyonidae	*Cynodictis exilis* Teilhard de Chardin, 1915	Subcomplete Cranium MNHN.F.Qu unnumbered	Phosphorites of Quercy Late Eocene/Early Oligocene
Amphicyonidae	*Cynodictis lacustris* Gervais, 1852	Complete cranium—New specimen MNHN.F.Qu 17762	Phosphorites of Quercy—Aubrelong 1 Late Eocene/Early Oligocene
Amphicyonidae	*Cynodictis lacustris* Gervais, 1852	Subcomplete Cranium MNHN.F.Qu 17502	Phosphorites of Quercy Late Eocene/Early Oligocene
Amphicyonidae	*Cynodictis lacustris* Gervais, 1852	Subcomplete Cranium MNHN.F.Qu 17765	Phosphorites of Quercy Late Eocene/Early Oligocene
Amphicyonidae	*Cynodictis peignei* Le Verger et al., 2020	Subcomplete Cranium MNHN.F.Qu 9007; MNHN.F.Qu 9008	Phosphorites of Quercy—Mouillac Late Eocene/Early Oligocene
Amphicyonidae	*Cynelos lemanensis* Pomel, 1846	Subcomplete Cranium Musée des Confluences—LA 85	Allier Basin—Billy Late Eocene/Early Oligocene
Amphicyonidae	*Cynelos lemanensis* Pomel, 1846	Rostrum and Basicranium University of Lyon—UCBL-FSL 65655	Allier Basin—Saint-Gérand-le-Puy Late Eocene/Early Oligocene
Amphicyonidae	*Pseudocyonopsis ambiguus* Filhol, 1876	Subcomplete Cranium MHNG V3272	Allier Basin—Saint-Gérand-le-Puy Late Eocene/Early Oligocene
Amphicyonidae	*Ysengrinia gerandiana* Viret, 1929	Subcomplete Cranium MNHN.F.Qu 1903–20	Allier Basin—Saint-Gérand-le-Puy Late Eocene/Early Oligocene
Amphicynodontidae	*Amphicynodon gracilis* Filhol, 1874	Complete cranium—New specimen MNHN.F.Qu 17763	Phosphorites of Quercy—Aubrelong 1 Late Eocene/Early Oligocene
Amphicynodontidae	*Amphicynodon* sp. Filhol, 1882	Rostrum MNHN.F.Qu unnumbered	Phosphorites of Quercy Late Eocene/Early Oligocene

Table 2 Cranial measurements (in mm) following Le Verger et al. (2020)

Species	SKL	OoL	SL	SW	SH	NL	NW	NH
Paramiacis exilis MNHN.F.Qu 8752	47	31	9	15	12	18	14*	12
Quercygale angustidens MNHN.F.Qu 8755	121	80	33	33	34	54	36	35
Palaeoprionodon lamandini MNHN.F.Qu 9348	69	48	15	18	17	34	25	20
Palaeoprionodon lamandini MNHN.F.Qu 9371	72	51	16	14*	19	36	25	24
Cynodictis exilis MNHN.F.Qu unnumbered	97	70	18	28	23	47	38*	31
Cynodictis lacustris MNHN.F.Qu 17762—New specimen	111	72	28	29	25	44	50	29*
Cynodictis lacustris MNHN.F.Qu 17502	102	72	28*	28	28	54	42*	30*
Cynodictis lacustris MNHN.F.Qu 17765	120*	87	–	–	–	78	40	35*
Cynodictis peignei MNHN.F.Qu 9007; 9008	107	68	31	30	28	52	44	36*
Cynelos lemanensis LA 85	280	160	100	70*	60	120	90*	100
Cynelos lemanensis UCBL-FSL 65655	250	160	90	70	50	100	90	90
Pseudocyonopsis ambiguus MHNG V3272	–	120	–	50*	60	70	80*	80
Ysengrinia gerandiana MNHN.F.Qu 1903–20	–	–	83	76	62	–	–	–
Amphicynodon gracilis MNHN.F.Qu 17763—New specimen	86	62	19	21	18	41	39	29
Amphicynodon sp. MNHN.F.Qu unnumbered	–	–	26	24	23	–	–	–

Symbols: *, estimations; -, Missing data

NH neurocranial height, *NL* neurocranial length, *NW* neurocranial width, *OoL* occiput to orbit length, *SH* snout height, *SKL* skull length, *SL* snout length, *SW* snout width

of Quercy (MNHN); UCBL, Université Claude Bernard Lyon.

Results

Systematic palaeontology

Carnivoramorpha Wyss & Flynn, 1993

Carnivoraformes Flynn, Finarelli, & Spaulding, 2010.

Carnivora Bowdish, 1821.

Amphicyonidae Trouessart, 1885

Cynodictis Bravard & Pomel, 1850

Cynodictis lacustris Gervais, 1852

Holotype—MNHN.F.Qu 8950, left mandible, with p2-m2, alveoli of p1 and m3.

Referred specimen—MNHN.F.Qu 17762, a cranium bearing right and left P2-M1, alveoli of I1-I3, canine, P1 and M2.

Locality—Aubrelong 1 (near Bach, Lot, France; Early Rupelian, MP21).

Note—MNHN.F.Qu 17762 was first assigned by Filhol (1876) as belonging to *Cynodictis intermedius*, without further clarification, although the genus diagnosis does not include cranial characters (Le Verger et al., 2020). Despite the absence of a mandible, the attribution of MNHN.F.Qu 17762 to *Cynodictis* is supported by the upper dentition with a P4 possessing a pointed and anteriorly placed protocone; an M1 with a well-developed parastyle and equally developed para-, meta-, and protocones, with a symmetrical and crescentic protocone showing pre- and post-protocristae leading to equally sized para- and metaconules, respectively, and with a strong posterolingual cingulum (Le Verger et al., 2020). Specific-level determination is made difficult within the genus *Cynodictis* due to a poor upper dentition record and cranial remains known for only three or potentially four of the six/seven species that comprises the genus: *Cynodictis exilis*, *Cynodictis lacustris*, *Cynodictis peignei*, and potentially *Cynodictis longirostris*. In agreement with the synonymy envisioned by Bonis (1978) and proposed by Kotsakis (1980) of the species *Cynodictis intermedius* with *Cynodictis lacustris*, we support a taxonomic reassignment of MNHN.F.Qu 17762 to *Cynodictis lacustris*. This attribution is further supported by the presence of a more strongly pronounced accessory cusp of P3 than in the other species; a wider protocone area of P4; a wider, longer M1 stylar shelf pointing more towards the cranial midline posteriorly; a broad transverse elongation of the zygomatic arches; a vertically oriented post-tympanic process of the squamosal; an intermediate width of the tensor tympani fossa and an intermediate position of the foramina for the ramus temporalis relatively to the sagittal crest between *Cynodictis exilis* and *Cynodictis peignei*, the latter having the widest tensor tympani fossa and foramina for the ramus temporalis, the closest to the sagittal crest; a narrow and shallow external acoustic meatus; and more strongly pronounced nuchal crests.

Comparative anatomical description

Sutures. Cranial bones of MNHN.F.Qu 17762 are not always well delineated. Visible sutures are mainly towards the front of the cranium: premaxilla, maxilla, nasal, frontal, palatine, lacrimal, orbitosphenoid, pterygoid, presphenoid, jugal, squamosal (zygomatic process and post-tympanic process), petrosal, and exoccipital bones are differentiable. The absence of some sutures, combined with complete tooth eruption and slight traces of wear on the teeth suggest that the individual was a young adult.

Dorsal view (Fig. 2A)—The rostrum has parallel edges, giving a rectangular shape, unlike *Ysengrinia gerandiana*.

The premaxilla extends well beyond the anterior part of the nasal, with a posterodorsal process reaching the level of the anterior margin of P2, unlike *Cynelos lemanensis*, where this process ends at the anterior margin of P3.

The maxilla extends to the orbit, and displays slight lateral bulges on its anterior part, corresponding to the root of the canines.

The infraorbital foramen, located at the level of the anterior edge of the P4, is wide and transversely stretched, contrary to *Amphicynodon gracilis*, for which the opening of the infraorbital foramen is rounded. Through this opening runs the infraorbital nerve, originating from the maxillary branch of the trigeminal nerve (CN V2), and which innervates several areas of the face (Fig. 3A). The depression formed between the lateral bulge and the infraorbital foramen could indicate the presence of a strong caninus muscle used to pull the upper lip and nasal wing for better nostril dilatation (Fig. 3C).

The nasal bones extend from the distal end of the rostrum, at the anterior edge of the canine, to the frontal bones into which they insert in a V-shape suture. The suture of the frontal, nasal and the maxillary bones has a W-shape. The posterior projection of the nasal is highly variable in the sample, but *Ysengrinia gerandiana*

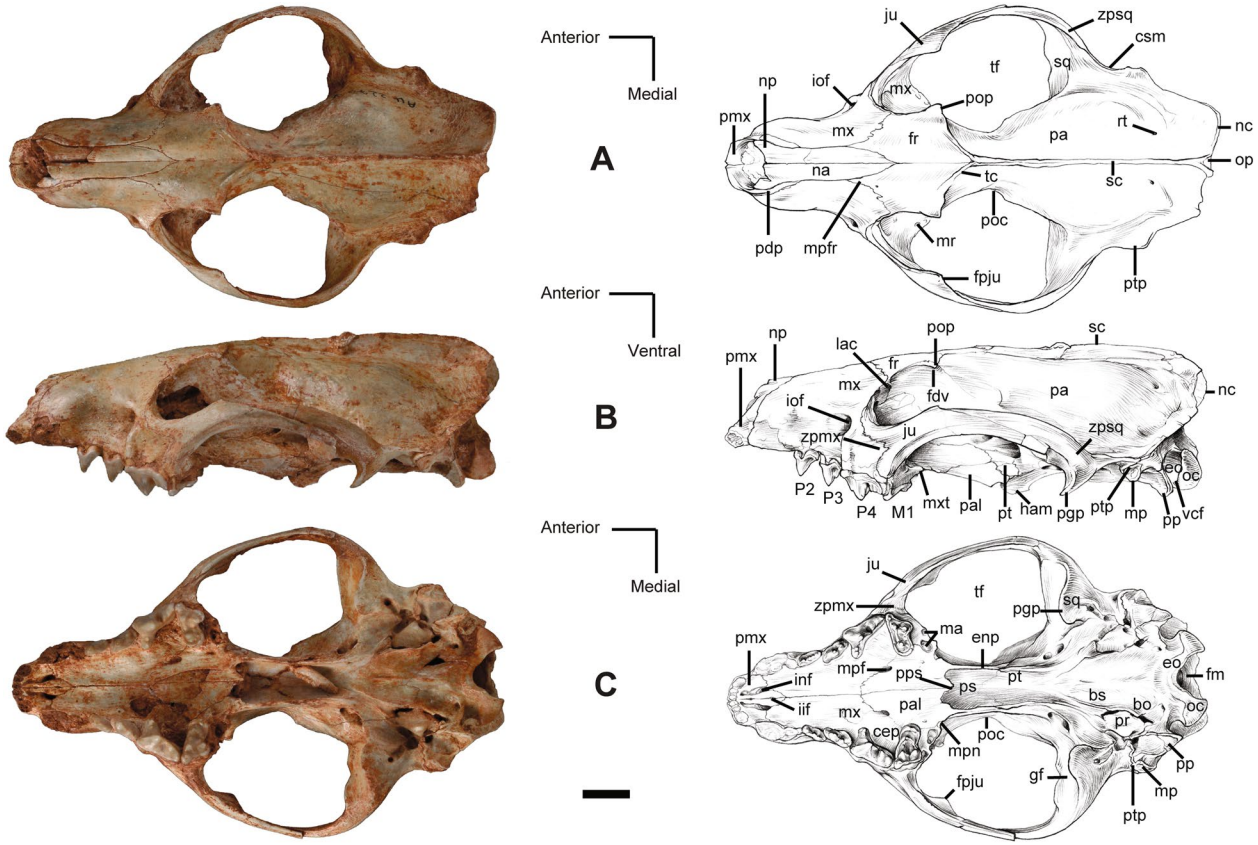

Fig. 2 Cranium of *Cynodictis lacustris* MNHN.F.Qu 17762 in dorsal (**A**), lateral (**B**), and ventral (**C**) views. Scale bar = 1 cm. *bo* basioccipital, *bs* basisphenoid, *cep* carnassial embrasure pit, *csm* crista supramastoideus, *enp* entopterygoid process, *eo* exoccipital, *fdv* frontal diploic vein foramen, *fm* foramen magnum, *fpju* frontal process of jugal, *fr* frontal, *gf* glenoid fossa, *ham* pterygoid hamulus; *iif* interincisive foramen, *inf* incisive foramen, *iof* infraorbital foramen; *ju* jugal, *lac* lacrimal, *M1* first upper molar, *ma* molar alveoli, *mp* mastoid process, *mpf* major palatine foramen, *mpfr* maxillary process of frontal, *mpn* minor palatine notch, *mr* molar root, *mx* maxilla, *mxt* maxillary tuberosity, *na* nasal, *nc* nuchal crest, *np* nasal process of nasal, *oc* occipital condyle, *op* occipital protuberance, *P2-4* second to fourth upper premolars, *pa* parietal, *pal* palatine, *pdp* posterodorsal process of premaxilla, *pgp* postglenoid process, *poc* postorbital constriction, *pop* postorbital process, *pp* paroccipital process, *pps* posterior palatine spine, *pmx* premaxilla, *pr* promontorium, *ps* presphenoid, *pt* pterygoid, *ptp* posttympanic process, *rt* foramen for ramus temporalis, *sc* sagittal crest, *sq* squamosal, *tc* temporal crest, *tf* temporal fenestra, *vcf* ventral condyloid fossa, *zpmx* zygomatic process of maxilla, *zpsq* zygomatic process of squamosal

exhibits the strongest difference with a more anteriorly terminated projection.

The frontal shows lateral bulges corresponding to the frontal sinuses, much more pronounced in *Cynodictis lacustris* than in the other amphicyonids examined. Frontal sinuses usually are involved in immune defence and/or air filtration by the nose, through the production of mucus. Anteriorly, the maxillary process of the frontal is strongly developed to the level of the infraorbital foramen. Posteriorly, this process is separated from the parietal by rather strong temporal crests. These crests originate at the level of the prominent and pointed postorbital process and shortly merge, slightly before the strongest constriction area of the postorbital. The postorbital constriction is also strong in *Pseudocyonopsis ambiguus*.

The orbitotemporal region is bordered laterally by the zygomatic arch, gently curved anteriorly and abruptly curved posteriorly. The zygomatic arch is composed, in equal proportions, of the jugal and the zygomatic process of the squamosal. The orbital fossa is much smaller than the temporal fenestra, which is significantly larger than that observed in the other crania studied. The posterior boundary of the orbit is marked by the frontal process of the jugal and the postorbital process, both of which being strongly developed and slightly curved into the temporal fenestra.

The zygomatic arch ends with the contact of the squamosal with the alisphenoid and parietal. The

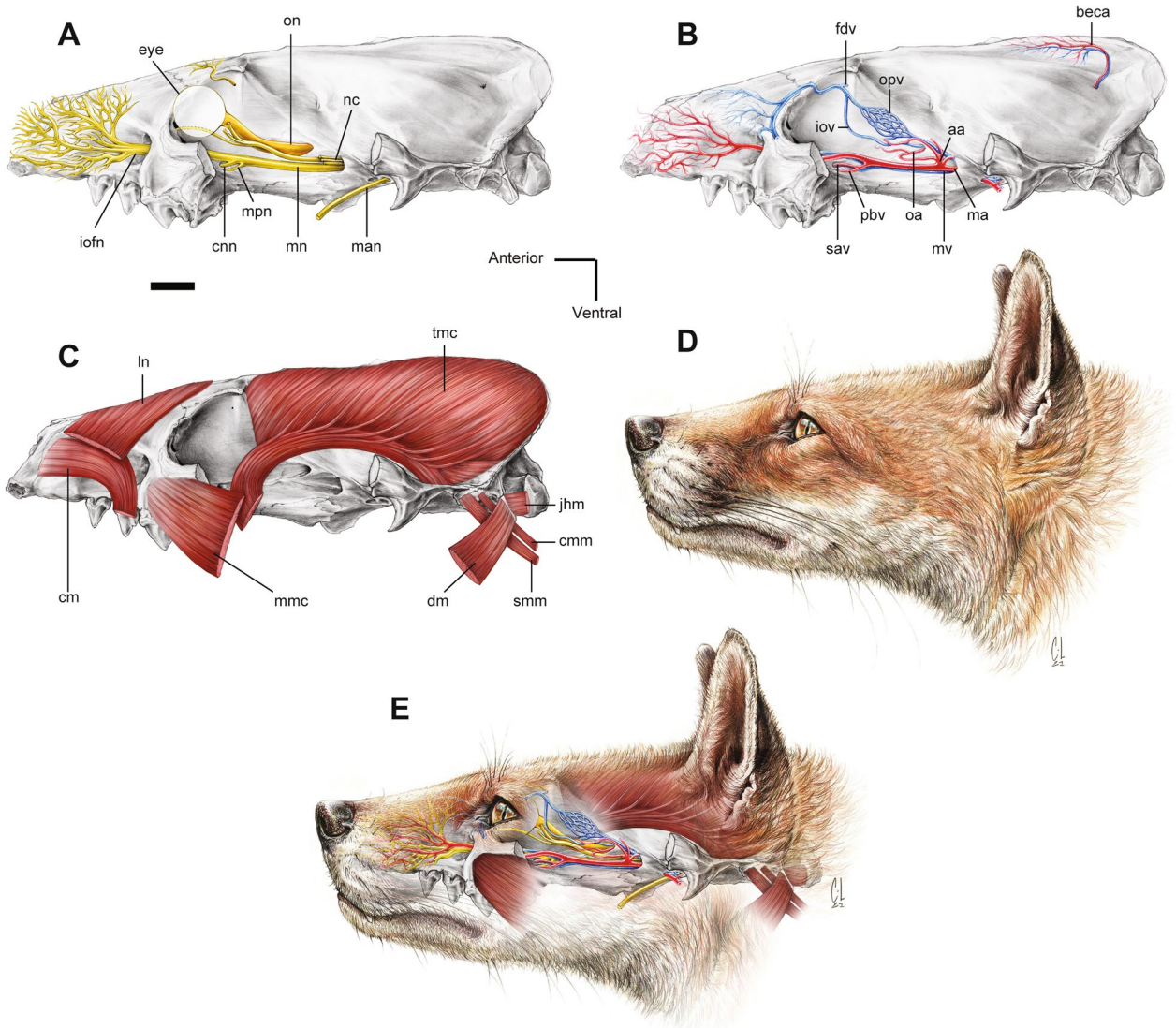

Fig. 3 Partial reconstruction of the innervation (**A**), vascularization (**B**), musculature (**C**) and entire head (**D**) of *Cynodictis lacustris* MNHN.F.Qu 17762 from the comparative description. (**E**) artistic vision grouping together all the reconstructions. Scale bar = 1 cm. *aa* anastomotic artery, *beca* branch of the external carotid artery, *cm* caninus muscle, *cmm* cleidomastoid muscle, *cnn* caudal nerve of the nasal, *dm* digastric muscle, *fdv* frontal diploic vein, *iofn* infraorbital nerve, *iov* internal ophthalmic vein, *jhm* jugulohyoid muscles, *ln* levator nasolabialis, *ma* maxillary artery, *man* mandibular nerve, *mmc* masseteric muscle complex, *mn* maxillary nerve, *mpn* major palatine nerve, *mv* maxillary vein, *nc* nerve complex, *oa* ophthalmic artery, *on* optic nerve, *opv* ophthalmic plexus vein, *pbv* palatine blood vessels, *sav* sphenopalatine artery and vein, *smm* sternomastoid muscle, *tmc* temporalis muscle complex

posteromedial termination of the arch is perpendicular to the anteroposterior axis and exhibits a marked and posteriorly curved crista supramastoidea. The concave curvature of the crista supramastoidea is weaker in *Cynelos lemanensis*. The crista supramastoidea reaches the posttympanic process of the squamosal, the latter extending posteriorly to the nuchal crests.

The nuchal crests have an oblique orientation with respect to the dorsoventral and anteroposterior axis. The nuchal crests are strongly elongated posteriorly to the point of completely obscuring the occipital condyles, in contrast to *Amphicynodon gracilis* in which they are smaller and almost vertical.

The sagittal crest of *Cynodictis lacustris* is high and long, occupying almost half of the total length of the cranium. The sagittal crest originates at the connection between the two temporal crests and reaches the connection between the two nuchal crests, corresponding to the occipital protuberance. In *Paramiacis exilis*, the sagittal crest is highly reduced, similar to *Amphicynodon gracilis*,

the closest taxon in the sample to the Amphicyonidae. The large size of the temporal fenestra and sagittal crest in *Cynodictis lacustris* suggests the presence of highly developed masticatory muscles (Fig. 3C).

The bulges of the parietal reflect the size of the endocranium. With a lyre-shape, the parietal bulges appear proportionally smaller than those observed in *Cynelos lemanensis* and *Amphicynodon gracilis*. The posterior aspect of these bulges that roughly correspond to the cerebral hemispheres occupy around 75% of the maximal width of the basicranium. An interspecific quantification of this aspect is impossible as half of the sample corresponds to incomplete crania.

In the posterior part of the cranium of *C. lacustris* and in the first third of its width, there is a well-marked foramen, on each side of the sagittal crest, which corresponds to the passage of the ramus temporalis, a branch of the external carotid artery supplying the temporalis muscle (Fig. 3B).

Lateral view and internal wall of the orbit (Figs. 2B, 4 and 5)—The cranium of *Cynodictis lacustris* is longer than tall, a proportion less marked in *Ysengrinia gerandiana*, in which the frontal is much higher and the rostrum comparatively shorter. The cranial height increases only slightly from anteriormost to posteriormost point as in *Cynelos lemanensis*, *Pseudocyonopsis ambiguus*, and *Amphicynodon gracilis*, suggesting an elongated attachment region for the levator nasolabialis muscle involved in upper lip lifting (Fig. 3C). However, *Amphicynodon gracilis* shows a shorter rostrum than *Cynodictis lacustris*, in which the maxilla is wider and slightly domed below the orbit. This maxillary area contains the maxillary sinus which acts as a thermal regulator and protector through the secretion of sinus mucosa.

The zygomatic process of the maxilla forms a bony tip that extends posteriorly into the jugal, giving a Y-shaped anterior termination. This Y-shape maxilla-jugal contact was not found in any other crania of the sample. In *Cynodictis*, this suture is at the level of M1 and not at the P4, unlike *Ysengrinia gerandiana*. Following the cranial musculature of *Canis familiaris*, this region formed by the maxilla-jugal contact probably served as an attachment for the masseteric muscle complex in *Cynodictis lacustris* (Fig. 3C).

The lacrimal, preserved on the right side of the cranium, is in contact with the frontal, maxilla, palatine and jugal. It is a small bone with conspicuous and wavy sutures, which contains a large lacrimal foramen corresponding to the opening of the nasolacrimal duct, a canal housing the Evans' duct and the lacrimal sac, whose function is to conduct tears to the eye (Fig. 3). More or less circular, the lacrimal foramen is located on the medial border of the jugal and above the maxillary foramen (= the internal opening of the infraorbital

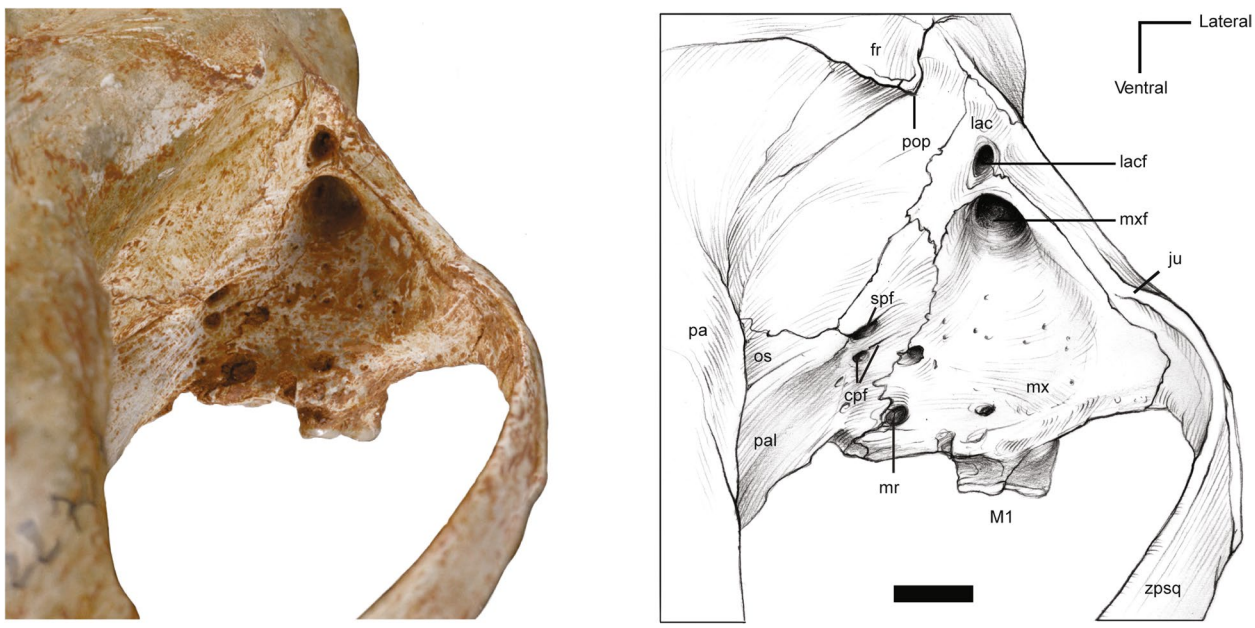

Fig. 4 Internal orbital wall of *Cynodictis lacustris* MNHN.F.Qu 17762. Scale bar = 1 cm. *cpf* caudal palatine foramen, *fr* frontal, *ju* jugal, *lac* lacrimal, *lacf* lacrimal foramen, *M1* first upper molar, *mr* molar root, *mx* maxilla, *mxf* maxillary foramen, *os* orbitosphenoid, *pa* parietal, *pal* palatine, *pop* postorbital process, *spf* sphenopalatine foramen, *zpsq* zygomatic process of squamosal

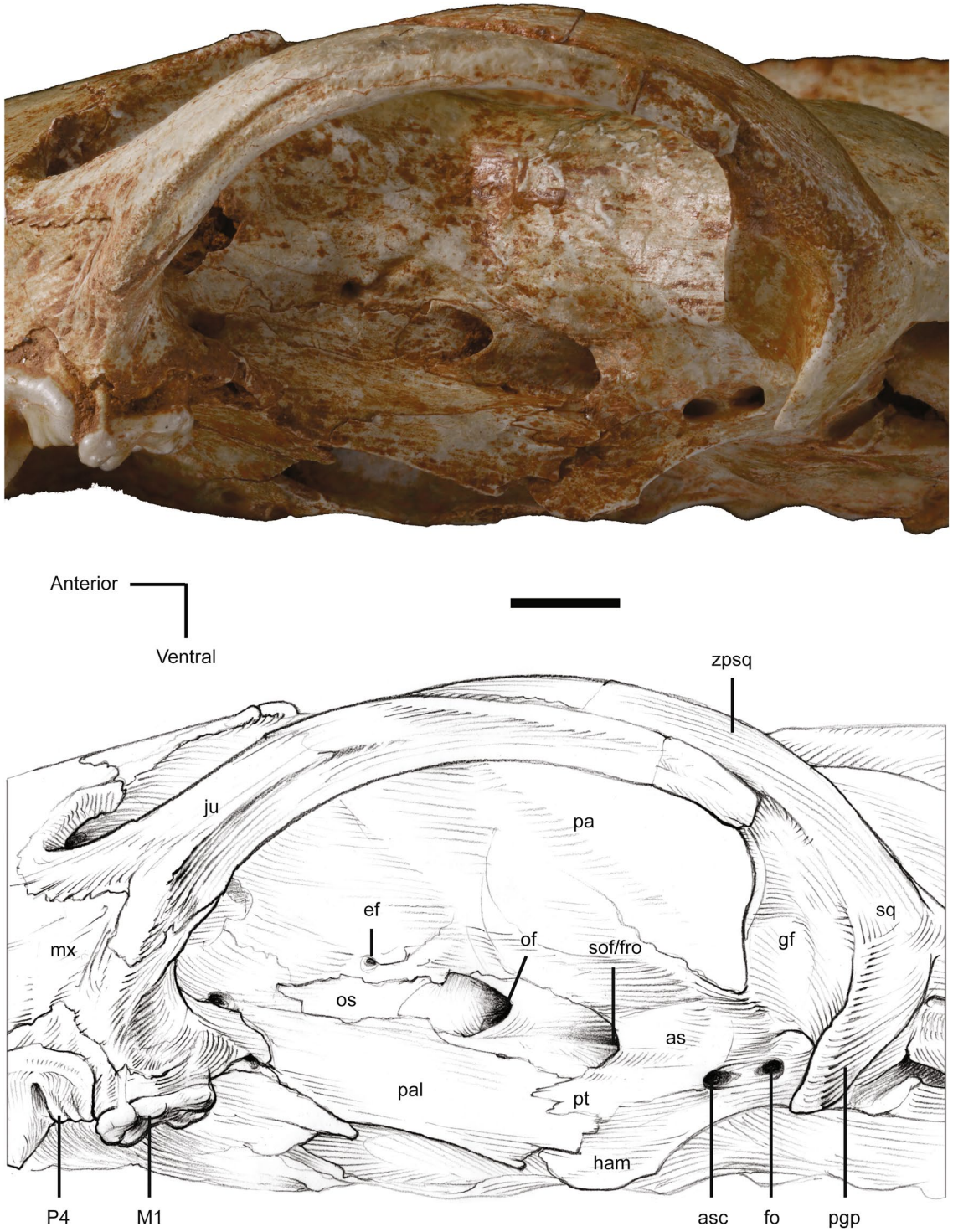

Fig. 5 Internal wall of the orbitotemporal region of *Cynodictis lacustris* MNHN.F.Qu 17762. Scale bar = 1 cm. *as* alisphenoid, *asc* alisphenoid canal, *ef* ethmoidal foramen, *fo* foramen oval, *gf* glenoid fossa, *ham* pterygoid hamulus, *ju* jugal, *M1* first upper molar, *mx* maxilla, *of* optic foramen, *os* orbitosphenoid, *P4* fourth upper premolars, *pa* parietal, *pal* palatine, *pgp* postglenoid process, *pt* pterygoid, *sof/fro* sphenorbital fissure/foramen rotundum, *sq* squamosal, *zpsq* zygomatic process of squamosal

foramen), which is about three times larger than the lacrimal foramen (Fig. 4).

Posterodorsally to the lacrimal and marking the posterodorsal limit of the orbit, the postorbital process forms a prominent peak. Ventral to the postorbital process, a tiny foramen for the frontal diploic vein is visible, although slightly marked (Fig. 3B). Only *Amphicynodon gracilis* exhibits a similar foramen, although located more anteriorly.

In the inner wall of the orbit, the maxilla is riddled with small and unidentified foramina, which are adjacent to three openings corresponding to the roots and alveoli of molars. More posteriorly, the maxillary tubercle is quite weak and does not contain all the roots of the M2 (not preserved on the specimen). Only *Cynelos lemanensis* and *Amphicynodon gracilis* show a well-marked maxillary tubercle.

The palatine, in its anteriormost part, at the junction with the lacrimal and maxilla, shows three foramina. The two ventralmost foramina correspond to the caudal ones of the palatine, for the passage of the major palatine nerve, a branch of the CN V2, and of blood vessels (Fig. 3A). Only *Amphicynodon gracilis* exhibits a single caudal foramen of the palatine, which is probably due to preservation bias. The third and most dorsal foramen corresponds to the sphenopalatine foramen, for the passage of the caudal nerve of the nasal, and the sphenopalatine artery and vein (Fig. 3B). In *Cynodictis lacustris*, the sphenopalatine foramen is wider than in the other taxa of the sample. These three foramina are involved in the innervation and vascularization of the rostrum (Fig. 3).

The pterygoid follows the palatine posteriorly. This cranial bone has a hook-shaped apophysis on its posteroventral part: the pterygoid hamulus.

Above the palatine and the pterygoid, the orbitosphenoid is visible in the internal wall of the temporal fenestra and exhibits three distinct foramina that grow in size anteroposteriorly. The first, located on the dorsal edge of the orbitosphenoid, corresponds to an ethmoidal foramen. In *Amphicynodon gracilis* and *Cynelos lemanensis*, the ethmoidal foramen is located more posteriorly. The second foramen, located at the contact between the alisphenoid and the orbitosphenoid, is the optic foramen for the passage of the optic nerve (CN II), the ophthalmic artery, and the internal ophthalmic vein (Fig. 3A, B). The third foramen, located behind the palatine on the alisphenoid, whose suture with the orbitosphenoid is not visible, corresponds to the merging of the superior orbital fissure, or sphenorbital fissure, and the foramen rotundum, which contains the rostral opening of the canal of the alisphenoid. In the former, many nerves and vessels pass (Fig. 3A, B): oculomotor (CN III), trochlear (CN IV), ophthalmic (CN V1), and abducens (CN VI) nerves, ophthalmic plexus vein, and anastomotic artery, which connects the maxillary artery and the polygon of Willis (complex of arteries providing vascularization to the encephalon). In the latter, the foramen transmits the maxillary nerve (CN V2), as well as the maxillary artery and vein, which function to innervate and vascularize the rostrum (Fig. 3).

On the most posteroventral part of the zygomatic arch, the postglenoid process is well marked and reaches the same height as the P3. It is slightly curved and points approximately 30° anteroventrally, forming the floor of the glenoid fossa. The postglenoid process exhibits strong interspecific variations. In *Cynelos lemanensis*, it has a less pronounced curvature, whereas, in *Amphicynodon gracilis*, it is smaller and much more curved forward. In contrast, *Pseudocyonopsis ambiguus* displays a strong postglenoid process.

Posteriorly, the squamosal exhibits a slightly marked process just posterior to the external acoustic meatus, the posttympanic process of the squamosal, which is oriented strongly anteroventrally. In an adjacent position of the latter, a half-smaller process projecting ventrally, the mastoid process of the petrosal bone, is present on which the long neck muscles, the sternomastoid and the cleidomastoid, involved in the mobility of the head, are attached (Fig. 3C). In *Cynelos lemanensis*, this process points laterally.

The mastoid process is followed posteriorly by the paroccipital process (=jugular process of Evans, 1993;=paracondylar process of the exoccipital of Wible & Spaulding, 2013). This prominent and posteroventrally projecting process serves as an attachment for the digastric (involved in the jaw movement) and jugulohyoid muscles (see Fig. 3C and Reighard & Jennings, 1935). In *Amphicynodon gracilis*, the paroccipital process is smaller, less wide, more pointed, and does not have an outward orientation of its inner side or a marked depression as in *Cynodictis lacustris*.

The exoccipital forms the ventral condyloid fossa between the paroccipital process and the occipital condyle. The latter is quite wide and oriented in the same way as the paroccipital process. Wider than high, the foramen magnum provides the articulation between the cranium and the atlas, the first cervical vertebra.

In the lateral view, the connection between the nuchal crest and the sagittal crest provides a wide muscle insertion shelf for the temporalis muscle (Fig. 3C).

Ventral view (Figs. 2C & 5)—The front of the rostrum is not completely preserved, and the premaxilla is not complete. Laterally, the premaxilla ends in front of the canines while its posterior extension forms a long bony process, stopping at the anterior third of the canine. The

premaxilla has two incisive foramina and one interincisive foramen. The formers are teardrop-shaped unlike in *Amphicynodon gracilis*, in which they are rounded. In *Ysengrinia gerandiana* and *Cynelos lemanensis*, they are more elongated than in *Cynodictis*. The incisive foramina allow the passage of the nasopalatine canal, which connects the oral and nasal cavities with the vomeronasal organ, of the nasopalatine nerve (a continuation from the CN V2) and of the rostral septal branch of the major palatine artery. The interincisive foramen is much smaller. Depending on the taxon considered, this foramen varies in size, position and may often be absent.

The palatine is partially damaged. The maxilla–palatine contact is slightly distinguishable, and begins at the anterior margin of the P4. Then, the palatine, rounded forward, forms a shelf delimited laterally by the M1. Its midline is slightly longer than that of the maxilla, contrary to *Ysengrinia gerandiana*. On the maxilla–palatine suture, laterally, the major palatine foramina are wide and located at the level of the contact between the P4 and M1. They transmit the palatine nerve, derived from the sphenopalatine branches of the CN V2, and blood vessels to the bony palate. Posteriorly, positioned medially to the M2 alveoli, a minor palatine notch is observable. A short posterior process of the palatine precedes the presphenoid; it is slight and not easily observable.

The presphenoid is followed by the pterygoid with which it forms a large and anteroposteriorly elongated fossa, of the width of the postorbital constriction and the length of the zygomatic arches. The fossa is bordered by the entopterygoid processes, nearly parallel bony rods, which end at about the posteromedial curvature of the zygomatic arch. In *Amphicynodon gracilis*, these processes are curved inwards. The pterygoid contacts the alisphenoid and basisphenoid.

Two foramina, large and in the same depression at the base of the alisphenoid, are visible laterally. The anterior one corresponds to the caudal opening of the alisphenoid canal, which allows the passage of the maxillary artery and vein in the alisphenoid canal until their exit through the foramen rotundum (Fig. 3B). The posterior one, oriented obliquely and opposite to the glenoid fossa, corresponds to the foramen ovale, for the passage of the mandibular nerve (CN V3) and an emissary vein (Fig. 3A, B). In *Canis familiaris*, sometimes a small notch marks the path of the middle meningeal artery from the maxillary artery (Evans, 1993). A similar feature is not observable for *Cynodictis lacustris*. In *Cynelos lemanensis*, these two foramina are almost fused.

Lateral to these foramina of the alisphenoid, the squamosal contains the glenoid fossa, which is elongated transversely and partly covered ventrally by the postglenoid process. The condylar process of the dentary articulates in this fossa.

The basisphenoid and the basioccipital are fused, and are delimited laterally by a muscular tubercle (sensu Evans, 1993; to which the longus capitis muscle is reportedly attached in the case of the domestic dog), showing a process posteriorly. The contact of the basisphenoid with the alisphenoid is not visible. Neither the tubercle nor the bony tip is visible on the other crania in the study. The basisphenoid has a lyre-shape and a slight crest along the midline. The basioccipital is hollowed laterally by strong depressions and shows the same less well-marked central crest. Only *Amphicynodon gracilis* exhibits marked differences with a basioccipital with much shallower depressions laterally and a much weaker midline crest ending in a bulge posteriorly. The basioccipital shows a raised rough surface, which corresponds to the area of attachment of the long head muscle (whose other end is attached to the cervical spine). The basioccipital ends at the contact of the exoccipital.

Auditory region (Fig. 6)—Posterior to the postglenoid process and distal to the lateral border of the cranium, the squamosal bears the postglenoid foramen, which transmits the postglenoid vein. The postglenoid foramen is positioned higher on the process in *Cynelos lemanensis*.

Posterior to this foramen and directed posteromedially to the tympanic cavity, a deep and narrow depression corresponds to the petrotympanic fissure (or Glaserian fissure). In this elongated fissure, the tympanic cord, a vegetative and sensory branch of the facial nerve (CN VII), connecting the latter to the lingual nerve (a sensory

(See figure on next page.)

Fig. 6 Auditory region of *Cynodictis lacustris* MNHN.F.Qu 17762 in ventral (**A**) and ventrolateral (**B**) views. Scale bar = 1 cm. *acf* aperture of cochlear fossula, *acrf* facet for anterior crus of ectotympanic, *ats*, sulcus for auditory tube, *bo* basioccipital, *boe* basioccipital excavation, *bs* basisphenoid, *cef* facet for caudal entotympanic, *cg* groove for internal carotid artery and nerves, *ci* crista interfenestralis, *ctp* caudal tympanic process, *dpn* foramen for deep petrosal nerve, *eam* roof of external acoustic meatus, *eo* exoccipital, *eot* exoccipital tubercles, *er* epitympanic recess, *fi* fossa incudis, *fv* fenestra vestibuli, *hf* hypoglossal foramen, *jf* jugular foramen, *mhf* facet for mallear hook of rostral process, *mp* mastoid process, *ms* mastoid shelf, *mt* muscular tubercle, *npc* groove for nerve of pterygoid canal, *pcrf* facet for posterior crus of ectotympanic, *pfac* pyriform fenestra with path for the internal carotid artery, *pgf* postglenoid foramen, *pgp* postglenoid process, *pp* paroccipital process, *pr* promontorium, *prb* promontorium bulge, *ptf* petrotympanic fissure, *ptp* posttympanic process, *rtp* rostral tympanic process of petrosal, *sf* stapedial foramen, *sff* secondary facial foramen, *sq* squamosal, *stf* stapedius fossa, *th* tympanohyal, *tpbs* tympanic process of basisphenoid, *tt* tegmen tympani, *ttf* tensor tympani fossa

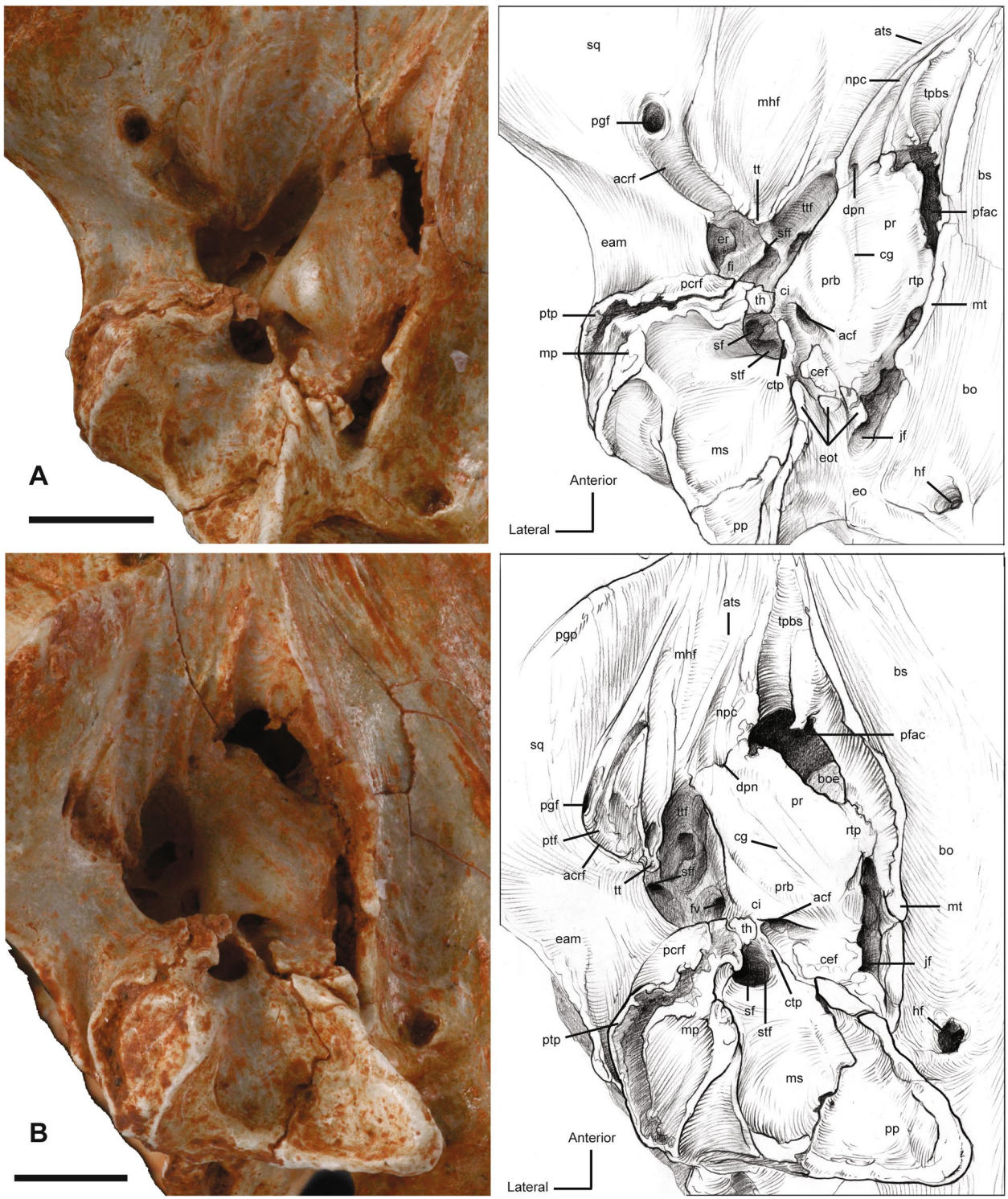

Fig. 6 (See legend on previous page.)

nerve derived from the mandibular nerve CN V3), is likely to circulate. In the dog, the tympanic cord indirectly innervates the submandibular and sublingual salivary glands and the anterior two-thirds of the tongue (Evans, 1993).

Medial to the petrotympanic fissure and bordering the tegmen tympani, a large anteroposteriorly stretched

depression likely constitutes a facet for insertion of the spine of the rostral process of the malleus (as described and illustrated in *Nandinia*, Wible & Spaulding, 2013).

Lateral to the petrotympanic fissure, a smaller but deeper depression just posterior to the postglenoid foramen received the anterior crus of the ectotympanic, the external component of the auditory bulla. This depression is much smaller in *Pseudocyonopsis ambiguus* and *Cynelos lemanensis*.

Near the external edge of this depression, a large and broad bony shelf formed by the squamosal corresponds to the roof of the external acoustic meatus through which sound travels to the tympanum. This shelf is slightly wider in *Pseudocyonopsis ambiguus* and *Cynelos lemanensis* than in *Cynodictis lacustris*. This shelf is followed posteriorly by the posttympanic process of the squamosal on which there is a facet for the insertion of the posterior crus of the ectotympanic. The posttympanic process is joined posteriorly by the mastoid process of the petrosal.

The petrosal is characterized in ventral view by a bean-shaped anterior part stretched anteriorly, the promontorium, and a posterior part forming a large bony "tongue", the mastoid part.

The promontorium is slightly roughened on its lateral and central surface. Its anterior extension is elongated and rounded anteriorly. The promontorium is crossed transversely by a slight groove over which the internal carotid artery circulated. The general morphology of the promontorium of *Cynelos lemanensis* is quite similar to that described in the Ursidae (Hunt, 1977). The promontorium of *Cynodictis lacustris* is pierced at its posterior base by two fenestrae: (1) the cochlear fossula opening, which contains the cochlear fenestra and received the secondary tympanic membrane; (2) anterodorsally to the bulge lateral to the cochlear fenestra, the vestibular fenestra, which is more dorsal and rounded, and housed the plate of the stapes and the annular ligament. The opening of the cochlear fossula, located posteromedial to the tympanohyal, is directed towards the mastoid shelf of the petrosal. The cochlear fenestra, within the cochlear fossula, is surmounted anteriorly by a bulge of the promontorium, resulting from the first turn of the underlying cochlea (=tympanic ramp). The latter is connected to the tympanic cavity by the secondary tympanic membrane, housed in the cochlear fenestra.

The posterior extension of the cochlear fossula forms a broad depression stretched across its width, and bordered laterally by a short process, interpreted here as the medial section of the caudal tympanic process of petrosal (sensu MacPhee, 1981). At its medial end, the cochlear fossula is bordered by a bony bulge that bears, only on the right side of the cranium, a small process marking a notch posterolateral to the cochlear fossula opening.

The vestibular fenestra, located anteriorly to the tympanohyal, opens towards the roof of the external acoustic meatus. The fenestra connects the ossicular chain with the vestibular ramp of the cochlea. These two openings are separated by a bulge: the crista interfenestralis. In *Pseudocyonopsis ambiguus*, these two fenestrae are closer together than they are in *Cynodictis lacustris*.

The mastoid part of the petrosal is bordered anterolaterally by the mastoid process, which forms a narrow shelf transversely and elongated ventrodorsally.

Anteromedially, a thin bony crest extends almost to the promontorium. This has a flat, circular facet joint at its medial end, the tympanohyal, which provides a connection between the tympanic cavity and the hyoid arch.

Posterior to the mastoid process, a bean-shaped bony lamina forms the exposed portion of the mastoid. It is bordered medially by a large, slightly concave to almost flat, and smooth mastoid shelf, which expands medially into the exoccipital with the prominent paroccipital process of the exoccipital. In *Amphicynodon gracilis*, this area containing the mastoid shelf and the paroccipital process of the exoccipital is considerably reduced. In *Cynelos lemanensis*, the area is narrower and longer. Pointing posteroventrally, the paroccipital process of *Cynodictis lacustris* is hollowed out on its inner side oriented anterolaterally. Two crests constitute the paroccipital process: the more mesial one starts from the apex of the process towards the cochlear fenestra while the more lateral one starts from the same point towards the apex of the mastoid process with a slight curvature.

The medial margin of the mastoid process forms a thin bony rod with a bulge in front of the cochlear fenestra. The bony rod corresponds to the lateral section of the caudal tympanic process of petrosal (sensu MacPhee, 1981), which adjoins the tympanohyal, forming a very round notch: the stylomastoid foramen. In the dog, the stylomastoid foramen marks the exit of the facial nerve and the stylomastoid artery (a branch of the caudal auricular artery) from the middle ear. Through this notch is visible, in ventral view, the stapedial fossa, which is deep, almost oval and the anterior wall of which is formed by the underlying lateral semicircular canal of the inner ear. The stapedial fossa indicates the location of the stapes and the stapedial muscle.

Anterolaterally and bordered medially by the promontorium, there is a wide and deep depression, slightly damaged. Its bony roof is formed in part by an epitympanic wing of the petrosal anteriorly, an epitympanic wing of the squamosal, and the tegmen tympani posteriorly. The most anterior and transversely oriented cavity is the fossa for the tensor tympani muscle, the second muscle of the tympanic cavity. This cavity is separated from a more posterior and rounded depression by a small bony

wall. This depression is hollowed out by two pits. The most anterior, the epitympanic recess, is also the widest. This recess is essential for the proper functioning of the ossicular chain and houses the malleus-incus joint. The most posterior pit, the fossa incudis, is twice as small but deeper than the epitympanic recess. The fossa incudis houses the short process of the incus and is located anterior to the stapedial fossa and separated from the latter by the crista parotica which forms a thick bony barrier. In *Cynelos lemanensis*, the epitympanic recess and the fossa for the tensor tympani appear proportionally smaller.

Medial to the epitympanic recess and fossa incudis is the damaged facial canal, which runs along the medial edge of the promontorium. This canal opens between the epitympanic recess and the vestibular fenestra to allow passage of the hyomandibular branch of the facial nerve (CN VII) via the secondary facial foramen. This major branch of the facial nerve originates from the geniculate ganglion contained in the supracochlear cavum, a space within the petrosal (thus not visible), located under the roof of the epitympanic recess or tensor tympani fossa.

On the medial edge of the promontorium and on the most medial part of the posterior bulge to the cochlear fossula, there are two clear facets, which contact the caudal entotympanic, an element of the auditory bulla. The more anterior and longer facet is carried by the rostral tympanic process of the petrosal. The bony bulge marking the posterior margin of the cochlear fossula is adjoined by three marked tubercles of the exoccipital. They define three sulci, the most posterior of which probably marks the passage of the auricular branch of the vagus nerve (CN X). This sulcus directly joins the facial nerve at its exit from the stylomastoid foramen.

Anteromedial to these three tubercles is a large foramen corresponding to the jugular foramen, indicating the passage of the auricular branch of the vagus nerve, the glossopharyngeal nerve (CN IX), accessory nerves, and the jugular vein. The jugular foramen is included in a long fissure that extends anteriorly between the promontorium and the basioccipital. This fissure is bordered by the long muscular tubercle of the basioccipital.

Posteromedial to the jugular foramen and piercing the exoccipital, the hypoglossal foramen is similar in diameter to the latter and marks the passage of the hypoglossal vein and nerve (CN XII), which function to innervate the tongue.

The anterior apex of the promontorium is separated medially from the basioccipital by a large hole, which may correspond to the pyriform fenestra (sensu MacPhee, 1981), or perhaps to the foramen lacerum of Evans (1993) (see the discussion in Wible & Spaulding, 2013). This orifice contains the foramen for the internal carotid artery. Anterior to this large fenestra, the tympanic process of the basisphenoid forms a large bony pocket. The large dorsal excavation of the basioccipital probably results from the presence of a well-developed inferior petrosal sinus. According to Hunt (1977), this anatomical feature is present only in some species of extant bears (*Ailuropoda melanoleuca* David, 1869; *Melursus ursinus* Shaw & Nodder, 1791; *Ursus americanus* Pallas, 1780; *Ursus arctos* Linnaeus, 1758), and Amphicyonidae—*Cynodictis lacustris* and *Cynelos lemanensis* possess, in fact, this deep excavation of the basioccipital. Hunt (1977) showed, moreover, that the large size of the pyriform fenestra and the strong excavation of the basioccipital are related to the particular circulation of the internal carotid artery, resulting from the common carotid artery and which reaches the auditory cavity rather posteriorly on the promontorium, at the level of the rostral tympanic process. This artery runs over the promontorium, accompanied by associated nerves, on which it forms a slight but wide sulcus that extends to the apex of the promontorium. Then, the internal carotid artery loops in the depression anterior to the apex of the promontorium, which is oval and located in the basisphenoid (or alisphenoid, these two bones being undifferentiated here) and enters the pyriform fenestra to the foramen of the internal carotid artery. In the four species of Ursidae with the basioccipital excavation, the internal carotid artery makes a second loop (called the "ursid loop") in the dorsal excavation of the basioccipital to continue its course toward the front of the cranium. Such an "ursid loop" circulation of the internal carotid artery is thus inferred for Amphicyonidae, as illustrated by Hunt (1977) for *Cynelos*.

Comprised between the tympanic process of the basisphenoid and the sulcus for the auditory bulla, a well-marked sulcus begins at a foramen anterior to the promontorium. This foramen marks the passage of the deep petrosal nerve, originating from the plexus of the internal carotid artery, which circulated in the sulcus and joined the greater petrosal nerve (the anterior branch of the facial nerve) to form the pterygoid canal nerve or Vidian nerve in the pterygoid canal. The sulcus for the pterygoid canal nerve ends at a foramen near the interior of the pterygoid crest and is located at the same transverse level as the foramen ovale.

Upper dentition (Fig. 7)—Despite the exceptional preservation of the specimen, the mandible was not found with the cranium. The incisors, canines, first premolars and second molars of the upper dentition are also missing.

Because of the sedimentary filling, the alveoli are difficult to interpret. Nevertheless, I3 are about three times wider than I1 and I2, with all incisors parabolically aligned, as in canids, in contrast to transverse alignment,

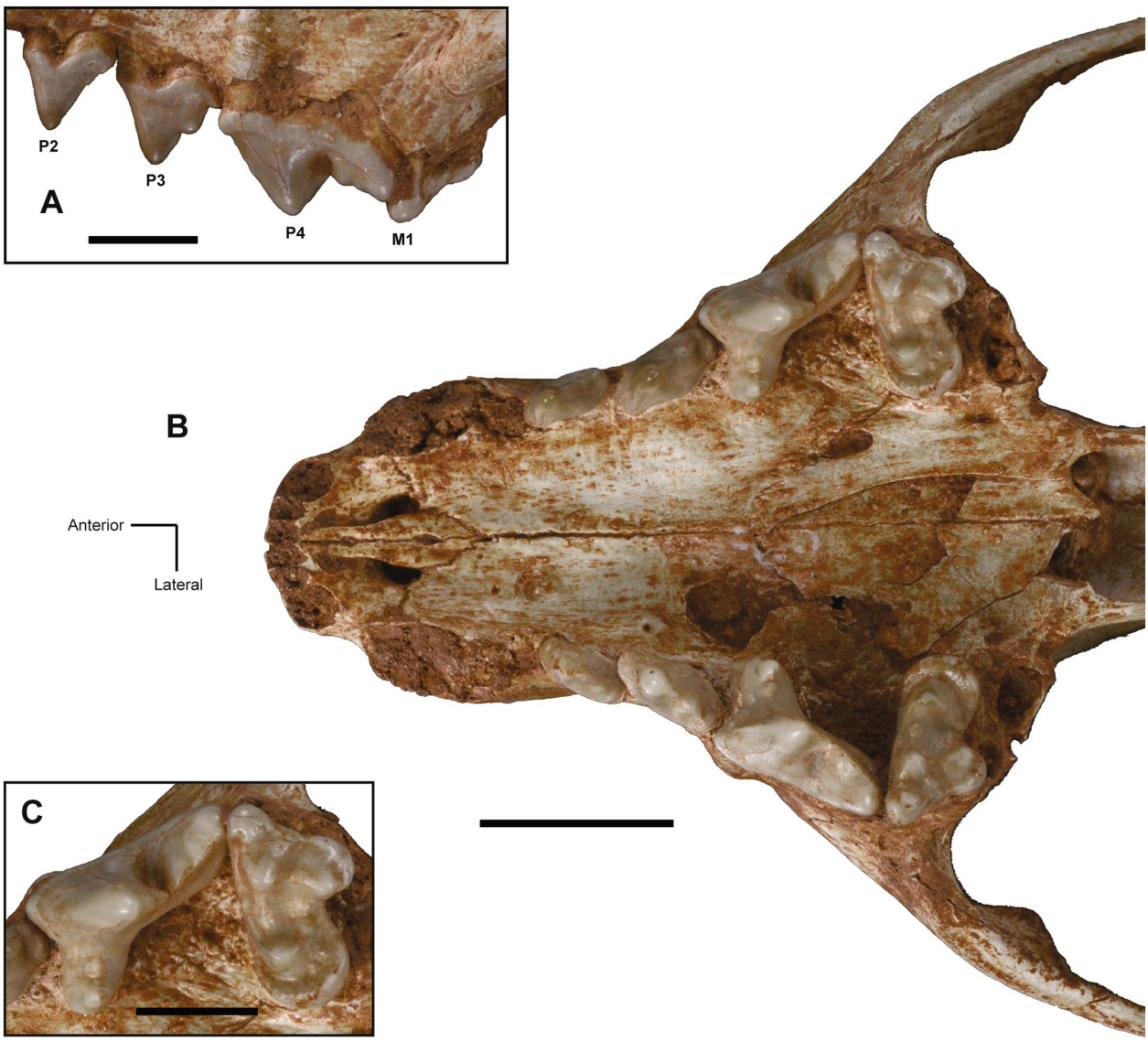

Fig. 7 Upper dentition of Cynodictis lacustris MNHN.F.Qu 17762 in labial (**A**) and occlusal (**B**,C) views. (**C**) is a close-up of the left P4 and M1. Scale bar = 1 cm. *M1* first upper molar, *P2-4* second to fourth upper premolars

as in felids (Biknevicius et al., 1996). This is also the case in *Cynelos lemanensis* and *Ysengrinia gerandiana*. A very small diastema separates them from the canines. The latter are the largest teeth according to the size of their alveoli. They are directly followed by the alveolus of the uniradiculate first premolar. In lateral view, from P2 to P4, the teeth are biradiculate, increasingly tall and long, and have an oblique orientation: the apex points towards the interior of the oral cavity.

The P2 is conical and has a single protruding cusp, the paracone. Its cingulum is thin, but almost complete. It forms a weak bulge mesially and a much stronger one distally. A crest connects the top of the cusp and the posterior bulge. *Ysengrinia gerandiana* has a much more massive, flattened P2 with a weak cingulum.

The P3 has the same characteristics as the P2 except that its two accessory cusps are more developed and individualized. The first one, rounded, is located posterior to the main cusp. They are connected by a short but well-defined crest. The second is much smaller and takes the place of the posterior bulge observed on P2. The morphology of the P2-3 of *Cynodictis lacustris* differs from that of other amphicyonids, for which accessory cusps are absent.

The P4, whose anterior root forms a bulge on the maxilla, has a cingulum forming an anterior bulge facing

forward and rising on the maxilla posteriorly. The main cusp, identified as the paracone, is the tallest in the entire dentition. The paracone is prominent and points backwards, with a posterior and an anterior crest that is less prominent than the former. The posterior crest comes into contact with the metastylar blade, which is long, protruding and has a very slight concave curvature in its center. Its contact with the paracone is more lingual in relation to the middle of the tooth, inducing an orientation of the metastylar blade towards the posterior part of the cranium. This contact produces a well-marked depression on the labial margin called the "carnassial groove". P4 has a relatively broad and lingually oriented talon that bears a strongly developed protocone and an accessory cusp that may correspond to the paraconule or metaconule. The P4-M1 contact produces a large triangular embrasure. None of the Amphicyonidae in the sample, except *Cynodictis lacustris*, has a paraconule on the P4 talon. One of the major differences observed between *Cynodictis* and *Cynelos* concerns the P4: it is smaller than the M2 and has a reduced protocone in *Cynelos lemanensis*, whereas the P4 is much larger in *Cynodictis lacustris*. In *Cynelos lemanensis*, a small crest descends on the medial part of the paracone, and a small crest descends from the paracone to the protocone.

In *Cynodictis lacustris*, the M1 is slightly rectangular, with a depression located at the posterior contact of the stylar shelf with the talon. The cingulum is quite developed around the stylar shelf and is even more so on the lingual margin of the talon where it forms a strong bulge as thick mesially as distally. It produces a well-marked crest in this area. The stylar shelf, which is much narrower than the talon, is oriented obliquely outward with respect to the anteroposterior axis and exhibits two cusps. The metastyle is poorly developed in contrast to the parastyle, which forms a prominent though strongly rounded cusp. The metacone is much lower than the paracone. They are both well developed and protruding. The centrocrista and preparacrista are more prominent than the postmetacrista. The talon is wide and points towards the interior of the oral cavity with a slight posterior inclination. The protocone is strong, protruding and offset mesially from the centre of the talon. The protocone is accompanied by a weakly developed paraconule and a slightly marked metaconule. The preprotocrista is more marked than the postprotocrista and rises towards the parastyle. Two thin crests are visible on the lingual base of the metacone and paracone. Two small bulges are present in the pit produced by the cingulum bulge.

There are many differences with the other amphicyonids of our sample. *Ysengrinia gerandiana* has a wider and more robust M1 (less tall and more flattened), rectangular rather than triangular in occlusal view. Its lingually oriented talon is thick and lacks a posterior depression; The cingulum is strong and does not form as prominent a crest on the talon; The preprotocrista, postprotocrista, and protofossa are pronounced, unlike the cusps; The protocone and metacone are not prominent but more rounded; The paracone is unfortunately broken in the specimen we examined. The M1 of *Pseudocyonopsis ambiguus* is similar to that of *Cynodictis lacustris*; However, the M1 has a posterior depression, unlike in *Cynodictis lacustris*; The talon widens to the stylar plate; The paraconule is stronger and well individualized while the metaconule is almost non-existent; The metacone is stronger than the paracone; Both cusps have anteroposterior crests. In *Pseudocyonopsis ambiguus* and in contrast to the condition in *Cynodictis lacustris,* the parastyle is much weaker, and is about the same level as the metacone. *Cynelos lemanensis* has an equilateral triangular M1. Its talon is V-shaped and has no preprotocrista, but a prominent postprotocrista; The protocone is protruding and V-shaped; The paracone is the tallest, as in *Cynodictis lacustris*; However, the parastyle is much less pronounced. Finally, the M1 of *Amphicynodon gracilis* is rectangular; It has an additional cusp compared to all the Amphicyonidae of the sample, the hypocone, which is well-marked and posterior to the protocone; The M1 cingulum on the lingual margin has a less prominent, shorter, and slightly crenulated crest; The parastyle does not form a cusp but rather a slightly serrated crest.

In *Cynodictis lacustris*, two small alveoli posterior to the talon of M1 indicate the presence of a biradiculated and highly reduced M2. The specimen shows no evidence of an M3, whereas the other amphicyonids in the sample all show an M2 and an M3. The overall dentition of *Cynodictis lacustris* is characterized by numerous sharp elements and a reduction of the grinding portion of the teeth. The dentition of *Cynodictis lacustris* was thus clearly sharp, more so than the other amphicyonids examined in this study.

Estimated size variation

The BM was estimated for 27 European Paleogene amphicyonid species (Table 3); the values range from about 2 kg (*Storchictis miacinus*) to 134 kg (*Crassidia intermedia*). The genus *Cynodictis* groups almost all the smallest taxa (4–12 kg), with the exception of *Storchictis miacinus* from the middle or late Eocene (Bonis, 2020), which is even lighter. Also, *Symplectocyon praecursor* (Amphicyonidae *incertae subfamiliae*; MP21) has a BM included within the range of *Cynodictis* spp. The heaviest taxa are thaumastocyonines, with two European representatives: *Ysengrinia tolosana* (~100 kg) and *Crassidia intermedia* (~134 kg). The BM of Haplocyoninae (four species) ranges from 26 to 86 kg. Compared to the

Table 3 Paleogene European amphicyonids with computation of Body mass, RBL and RPS values, and inferred diets

Family	Species	MP/Age	Body mass (kg)	RBL	RPS	Inferred diet
Stem amphicyonid	*Cynodictis cayluxensis* Filhol, 1876	Late Eoc.- early Oligoc	12	–	0.809	Hypercarnivore
Stem amphicyonid	*Cynodictis crassus* Teilhard de Chardin, 1915	Late Eoc.- early Oligoc	11	1.893	0.769	Hypercarnivore
Stem amphicyonid	*Cynodictis exilis* Teilhard de Chardin, 1915	Late Eoc.- early Oligoc	4	1.902	0.702	Mesocarnivore
Stem amphicyonid	*Cynodictis ferox* Filhol, 1876	Late Eoc.- early Oligoc	10	1.874	-	Mesocarnivore
Stem amphicyonid	*Cynodictis lacustris* Gervais, 1852	MP18-21	7	1.914	0.691	Mesocarnivore
Stem amphicyonid	*Cynodictis longirostris* Filhol, 1872	Late Eoc.- early Oligoc	9	2.031	0.726	Hypercarnivore
Stem amphicyonid	*Cynodictis peignei* Le Verger et al., 2020	Late Eoc.- early Oligoc	7	1.702	0.727	Mesocarnivore
Stem amphicyonid	*Storchictis miacinus* Bonis, 2019	?Middle/late Eoc	2	1.942	0.567	Mesocarnivore
Undefined	*Amphicyanis felinoides* Springhorn, 1977	?Early/middle Oligoc	39	–	0.754	Hypercarnivore
Amphicyoninae	*Cynelos crassidens* Filhol, 1874	MP28-29	24	1.797	0.7	Mesocarnivore
Amphicyoninae	*Cynelos lemanensis* Pomel, 1846	MP28-30	42	1.837	0.698	Mesocarnivore
Amphicyoninae	*Cynelos rugosidens* Schlosser, 1899	MP26	37	–	0.694	Mesocarnivore
Amphicyoninae	*Goupilictis minor* Dehm, 1935	MP28-29	13	1.862	0.65	Mesocarnivore
Amphicyoninae	*Pseudocyonopsis ambiguus* Filhol, 1876	MP26-28	45	2.243	0.762	Hypercarnivore
Amphicyoninae	*Pseudocyonopsis antiquus* Helbing, 1928	MP21-23	29	1.461	0.663	Hypocarnivore
Amphicyoninae	*Pseudocyonopsis landesquei* Helbing, 1928	MP26-29	73	1.917	0.65	Mesocarnivore
Amphicyoninae	*Pseudocyonopsis quercensis* Ginsburg, 1965	Early Rupelain	38	2.21	0.863	Mesocarnivore
?Amphicyoninae	*Brachycyon gaudryi* Ginsburg, 1966	Rupelian	45	2.271	0.762	Hypercarnivore
?Amphicyoninae	*Harpagocyon inusitatus* Springhorn, 1977	MP30	35	–	–	–
?Amphicyoninae	*Pseudamphicyon lupinus* Schlosser, 1887	Rupelian	32	2.578	0.829	Hypercarnivore
?Amphicyoninae	*Symplectocyon praecursor* Springhorn, 1977	MP21	7	–	–	–
Haplocyoninae	*Haplocyon crucians* Filhol, 1879	MP29-30	45	1.794	0.655	Mesocarnivore
Haplocyoninae	*Haplocyon dombroskyi* Dombroski, 1888	MP29-30	45	1.822	0.708	Mesocarnivore
Haplocyoninae	*Haplocyon elegans* Bonis, 1966	MP29-30	26	1.79	0.724	Mesocarnivore
Haplocyoninae	*Haplocyonopsis crassidens* Bonis, 1973	MP30	86	2.006	0.615	Mesocarnivore
Thaumastocyoninae	*Crassidia intermedia* Meyer, 1849	MP29-30	134	–	0.715	Mesocarnivore
Thaumastocyoninae	*Ysengrinia tolosana* Noulet, 1876	MP29-30	107	1.771	0.739	Mesocarnivore

Symbol: -, missing data

Eoc Eocene, *MP* Mammalian Paleogene, *Oligoc* Oligocene, *RBL* Relative Blade Length, *RPS* Relative Premolar Size

Thaumastocyoninae and Haplocyoninae, Amphicyoninae were most diversified in Europe during the Oligocene with at least eight representatives, which exhibited much lower values compared to those of Haplocyoninae, with a BM comprised between 13 kg (*Goupilictis minor*) and 73 kg (*Pseudocyonopsis landesquei*). From the late Eocene to the end of the Oligocene, amphicyonids show a constant trend towards an increase of their maximum BM. In the Priabonian, the maximum BM is 12 kg (*Cynodictis cayluxensis*), while it reaches 45 kg during the Rupelian (*Brachycyon gaudryi*) and up to 134 kg at the end of the Chattian (*Crassidia intermedia*). The evolution of the minimum BM of European amphicyonids is harder to reconstruct as the exact stratigraphic distribution of the earliest amphicyonids, *i.e. Cynodictis* spp., is unknown (Kotsakis, 1980; Le Verger et al., 2020). If we consider that *Cynodictis* is not present in Europe after MP21, the minimum BM is therefore 2 kg during the Priabonian (*Storchictis miacinus*), 7 kg in MP21, 29 kg after MP21 (*Pseudocyonopsis antiquus*; MP21-23), but 13 kg at the end of the Chattian (*Goupilictis minor*). The Chattian thus possibly records the reappearance of small (< 20 kg) amphicyonids. If *Cynodictis* (*e.g.*, *Cynodictis lacustris*) was present during a long period in the Rupelian (*i.e.*, after MP21), it would imply that the mean BM of the amphicyonids remains somewhat constant during the Oligocene, around 7–15 kg. In this hypothesis, *Goupilictis minor* would not mark the reappearance of small amphicyonids.

Diet spectrum

The RPS and RBL values estimated for 25 amphicyonids from the late Eocene and Oligocene of Europe allow us to recognize three groups in the sample: 17 mesocarnivores, seven hypercarnivores, and one hypocarnivores (no bone-crushing mesocarnivore or scavenger amphicyonid is known in the European Paleogene; Fig. 8; Table 3). The sole hypocarnivore (*Pseudocyonopsis antiquus*) is recorded in the Rupelian. The hypercarnivores are numerous in the Priabonian and the Rupelian, with six species known, including three *Cynodictis* species (*Cynodictis cayluxensis*, *Cynodictis crassus*, and *Cynodictis longirostris*). Only one hypercarnivore is known for the Chattian (*Pseudocyonopsis ambiguus*). Amphicyoninae includes two hypercarnivores—*Pseudocyonopsis ambiguus*, *Brachycyon gaudryi*—and Haplocyoninae only one—*Pseudamphicyon lupinus*. Thaumastocyoninae is represented only by mesocarnivores. Van Valkenburg (2007) observed that the carnivorans represent a mammalian clade in which convergence is evident in the iterative appearance of ecomorphological varieties. The amphicyonids are no exception to this aspect: they show

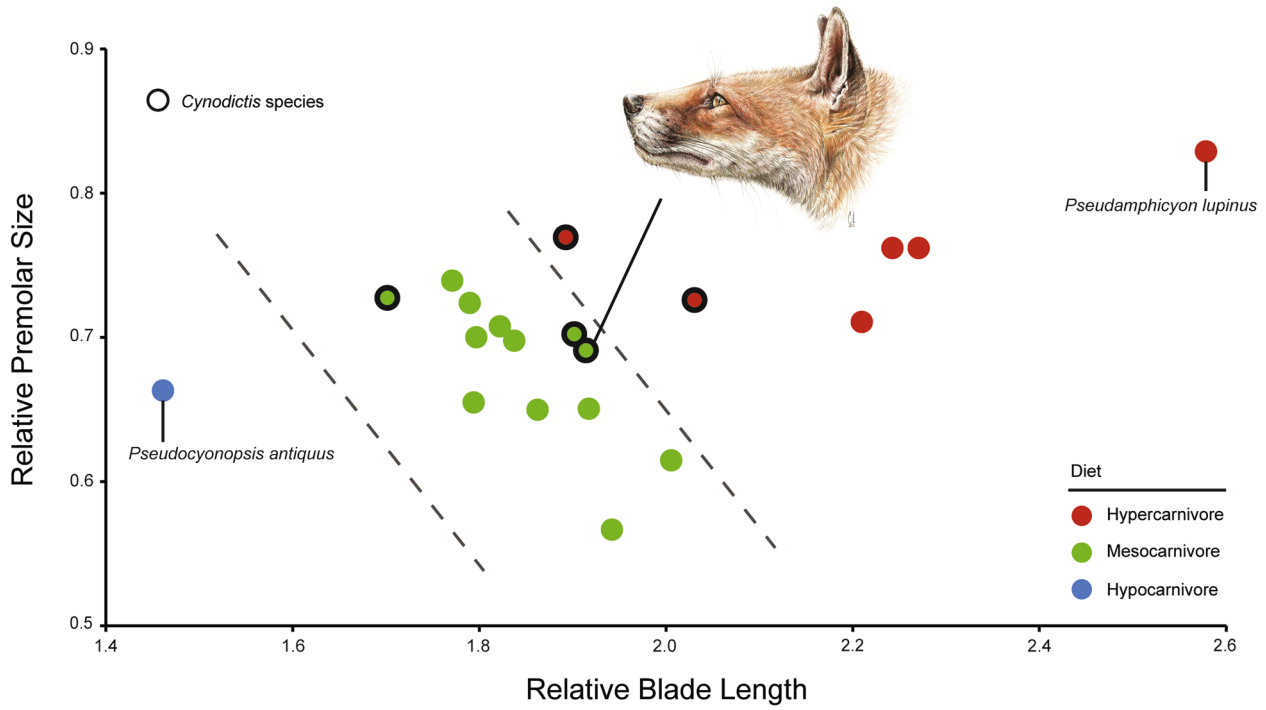

Fig. 8 Relative Premolar Size (RPS) in relation to the Relative Blade Length (RBL) with the different grouping for diet inferences. For more details on RPS and RBL computation, please refer to Table 3 and Table S1. The reconstruction corresponds to the studied specimen *Cynodictis lacustris* MNHN.F.Qu 17762

ecomorphologies adapted to a broad range of carnivore niches throughout the Paleogene. Moreover, *Cynodictis* shows that even the earliest amphicyonids were ecologically diverse: this genus indeed gathers mesocarnivorous and hypercarnivorous species.

Discussion

Cranial anatomy and notes on the origin of early European amphicyonids

The new specimen described in the present study is the most complete and oldest cranial remain of an amphicyonid from Europe. Amphicyonidae are first recorded in Europe in MP18 localities (*e.g.*, Sainte-Néboule, France; Priabonian) (Bonis, 1978). Their representatives from the Priabonian were usually referred to the genus *Cynodictis* (Bonis, 1978; Le Verger et al., 2020). A second genus—*Storchictis*—has been described based on a mandible from the Phosphorites of Quercy by Bonis (2020). Due to its small size, plesiomorphic morphology, and because the oldest fossils ever found in the phosphorites are dated to middle Eocene (Astruc et al., 2000), this monospecific genus was suggested to come from either the middle Eocene or the late Eocene (Bonis, 2020), arguments also valid for *Cynodictis*. The new cranium described in the present study provides an opportunity to re-discuss the retention of plesiomorphic characters within European taxa, especially because of its completeness.

The geographic origin of the earliest amphicyonids remains uncertain. The oldest known amphicyonids are recorded in North America, with *Daphoenus*, *Angelarctocyon*, and *Gustafsonia* (Tomiya & Tseng, 2016). Because of the lack of direct terrestrial connection between Europe and North America since the Lutetian due to the interruption of the Euramerican land bridges (*i.e.*, De Geer route and Thulean route; Rose, 2006), the earliest European amphicyonids might have arrived from North America through Asia. Nonetheless, the Asian fossil record of amphicyonids is extremely sparse and only few specimens have been reported for the Paleogene. These are for the Middle Eocene of Asia, *Cynodictis* in the Lushi Basin (China; Chow et al., 1973) and 'cf. *Cynodictis*' in the Ulan Shireh Formation (Inner Mongolia, China, Russell & Zhai, 1987). Tsubamoto et al. (2006) also referred a canine and a possible m1 talonid from the late-Middle Eocene of Myanmar to Amphicyonidae. The earliest unequivocal Asian Eocene amphicyonid occurrences are from the late Eocene of China and Mongolia: *Guangxicyon* from the latest Eocene of the Bose Basin (Guangxi, China; Zhai et al., 2003) and Amphicyonidae gen. et sp. indet. from the late Eocene Ergilin Dzo Formation (Mongolia; Egi et al., 2009). Because *Guangxicyon* is aberrant (strong brachygnathism with single-rooted p1-p2 and m2-m3 but without any dental loss), the relationships of this genus with other amphicyonids are difficult to decipher. Likewise, *Lonchocyon* from the late Eocene of the Erlian Basin (Inner Mongolia, China; Zhang et al., 2023), a potential ursid or an amphicyonid, is characterized by highly reduced premolars and m2-m3. The hypothesis that the earliest European amphicyonids migrated from Asia during the Priabonian, although supported by a parallel dispersion of *Hyaenodon* (Bastl et al., 2014; Lange-Badré, 1979), is therefore difficult to test because of a scarce fossil record.

The specimen described herein (MNHN.F.Qu 17762) is crucial for reconstructing the evolution of amphicyonids, as otherwise the group is abundant in the fossil collection from Phosphorites of Quercy but mainly represented by isolated dental elements (Bonis, 1978; Kotsakis, 1980; Le Verger et al., 2020; Solé et al., 2021; Springhorn, 1977; Teilhard de Chardin, 1915). *Cynodictis lacustris* can be characterized as follows:

(1) In the overall shape of the cranium: a rostrum with parallel edges, giving a rectangular shape, unlike *Ysengrinia gerandiana*; a cranium more elongated than high in contrast to *Ysengrinia gerandiana*, in which the frontal is much higher and the rostrum comparatively shorter, the cranial height increasing only slightly from anteriormost to posteriormost point as in *Cynelos lemanensis* and *Pseudocyonopsis ambiguous*; a distinctive anterior extension of the maxillary process of the frontal to the level of the infraorbital foramen; a unique Y-shaped maxilla-jugal contact; and cerebral hemispheres of the endocranium appearing proportionally smaller than those observed in *Cynelos lemanensis*.
(2) In the auditory region: an epitympanic recess and a fossa for the tensor tympani larger than in *Cynelos lemanensis*; a deep excavation of the basioccipital related to the particular circulation of the internal carotid artery called "ursid loop" present also in *Cynelos lemanensis*.
(3) In cranial sinuses: a more pronounced lateral bulges in the frontal than in the other amphicyonids, corresponding to the frontal sinuses usually involved in immune defense and/or air filtration; and a maxilla wider and more domed below the orbit than in the early ursids (here *Amphicynodon gracilis*), containing the maxillary sinus as a thermal regulator and protector through the secretion of sinus mucosa.
(4) In face innervation: a wider sphenopalatine foramen than in other taxa, suggesting a high innervation of the rostrum, and more specifically of the palate.
(5) In masticatory muscles: a strong postorbital constriction coupled with a large temporal fenestra, a

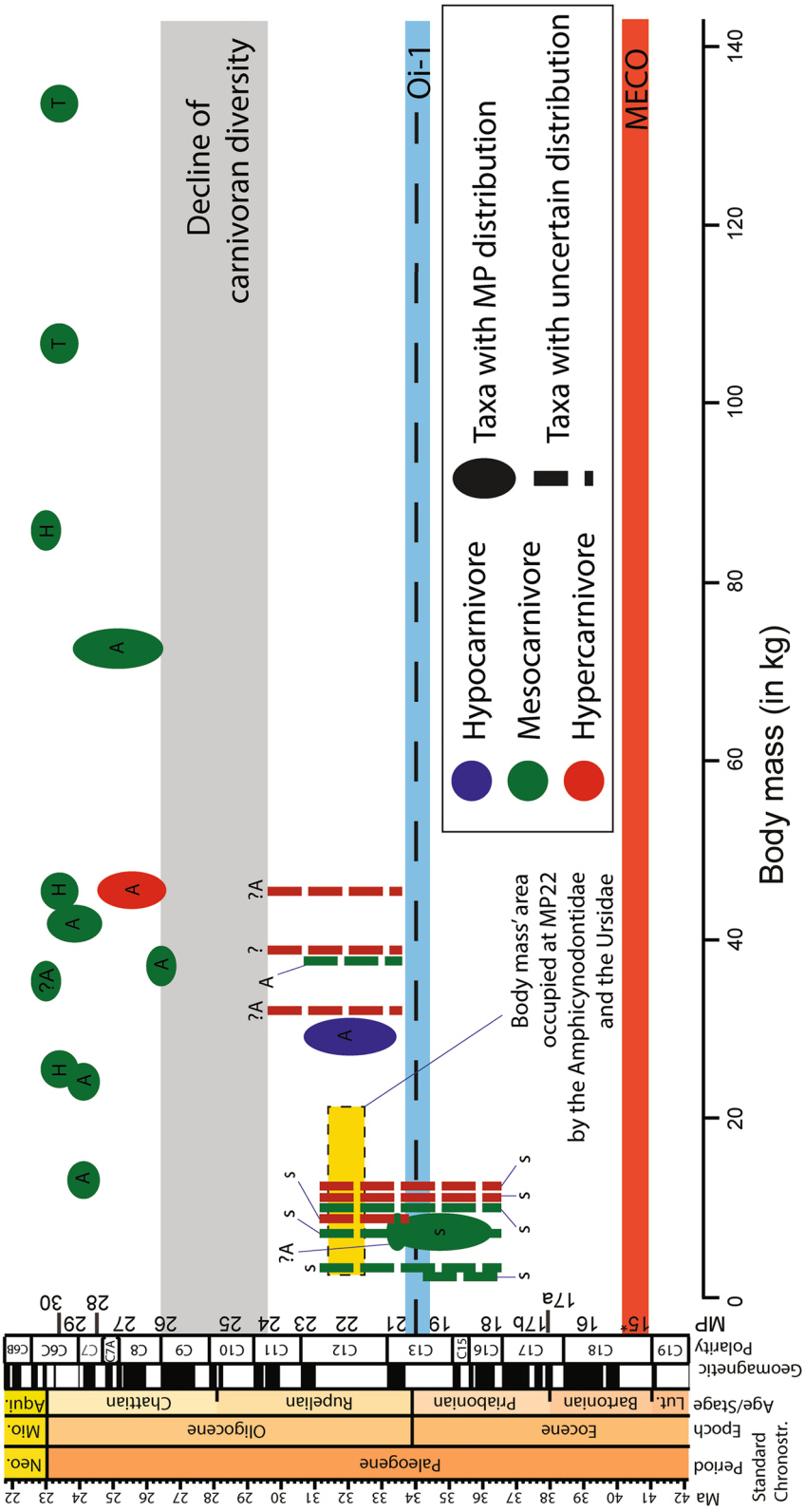

Fig. 9 Temporal distribution and the evolution of body mass and diet in European amphicyonids during the Paleogene. The values are available in the Tables 1 and 3, and Table S1. *A* Amphicyoninae, *Aqui* Aquitanian, *Chronostr* Chronostratigraphy, *H* Haplocyoninae, *Lut* Lutetian, *MECO* Middle Eocene Climatic Optimum, *Mio* Miocene, *Neo* Neogene, *Oi-1* Oligocene Glaciation Event, *S* early-diverging amphicyonid, *T* Thaumastocyoninae

small orbital fossa, and a well-marked posterior orbital boundary (following the postorbital process and the frontal process of the jugal) support the presence of relatively larger masticatory muscles than in other sampled amphicyonids; the high and elongated sagittal and nuchal crests provide a wide muscle attachment shelf for the temporalis muscle, far more developed than in the carnivoraform *Paramiacis exilis*, and in the early ursid *Amphicynodon gracilis*.

(6) In long neck muscle: a well-marked mastoid process of the petrosal bone, a highly pronounced paroccipital process with a marked depression, and tubercules on the ventral surface of the basisphenoid and the basioccipital, all supporting the presence of strong neck muscles in comparison to *Amphicynodon gracilis*.

On the evolution of European amphicyonids during the Paleogene

The ecological evolution of amphicyonids in Europe has previously been reconstructed for the Miocene only (Solé et al., 2022b; Viranta, 1996). Here, we provide a wider view of how these predatory mammals ecologically and taxonomically evolved in Europe during the Paleogene (Fig. 9). The two earliest European amphicyonids, *Cynodictis* (7 species; Bonis, 1978; Kotsakis, 1980; Le Verger et al., 2020) and *Storchictis* (monospecific; Bonis, 2020), had low BMs: between 2 and 12 kg. However, their diets were varied, with 3 hypercarnivores and 5 mesocarnivores. Because of its small size, two potential diets, and cranial morphology, the genus *Cynodictis* can be regarded as a fox-like or bush dog-like predator depending on the species (Van Valkenburgh, 1991).

A crucial question is whether this first fauna of amphicyonids (i.e., *Cynodictis* and *Storchictis*) survived the '*Grande Coupure*' or not. This great faunal shift (Legendre & Hartenberger, 1992; Stehlin, 1909; Weppe et al., 2023), which is coeval with the global climate cooling called the Oligocene Oi-1 event (Zachos et al., 2001), is marked by numerous disappearances in various vertebrate groups, but also many appearances. The '*Grande Coupure*' has had a profound impact on the European carnivorous mammal fauna (Solé et al., 2022a). The new cranium of *Cynodictis lacustris* described here raises questions about the survival of amphicyonidae across the '*Grande Coupure*', since this species is known from the Priabonian (MP18) (Bonis, 1978), the Aubrelong specimen is dated to MP21, and younger *Cynodictis* are not well-dated from the Phosphorites of Quercy. In accordance with Costa et al. (2011), the oldest part of MP21 corresponds to the tail end of the '*Grande Coupure*', thus supporting the presence of *Cynodictis lacustris* towards the end of the event and potentially a survival of the species at this great faunal shift. Our finding thus questions the previous statements that amphicyonids and *Cynodictis* in particular did not cross the '*Grande Coupure*' (Bonis, 2020), and that Oligocene amphicyonids could only be Asiatic migrants as could artiodactyls (Weppe et al., 2023). *Cynodictis lacustris* is thus peculiar, perhaps joining two species of *Hyaenodon* (Hyaenodonta) as the only predatory species crossing the '*Grande Coupure*' (Lange-Badré, 1979). At the opposite, endemic hyaenodonts and carnivoraforms, as well as hyainailourines (Hyaenodonta), disappeared from Europe at that end of the Priabonian (Solé et al., 2022a).

The presence of another potential amphicyonid (*Symplectocyon praecursor*) with BM (7 kg) similar to that of *Cynodictis lacustris* in the MP21, and the absence of small amphicyonid in the MP22 (Bonis et al., 2019; Peigné et al., 2014), suggest that amphicyonids of small sizes did not exist in younger MP levels. In some of the fossil-rich localities in MP22 (Mas de Got, La Plante 2, Valbro), amphicynodontids (early ursid) are abundant, with *Pachycynodon* and *Amphicynodon*, and the ursid *Cephalogale* (Bonis et al., 2019). The estimated BM of these predators ranges from 3 to 21 kg (Table S1, Fig. 9), which overlaps with the range of the early amphicyonids. It is thus probable that the *Cynodictis*-like amphicyonids survived the '*Grande Coupure*' but went to be quickly ecologically replaced by Amphicynodontidae and Ursidae (around MP21-22).

The large amphicyonids of the MP21 range from 29 kg (*Pseudocyonopsis antiquus*) to 45 kg (*Brachycyon gaudryi*; Fig. 9), and display a diversity of diets with one mesocarnivore, one hypocarnivore, and three hypercarnivores. This is the sole period where a hypocarnivorous amphicyonid (*Pseudocyonopsis antiquus*) is recorded in Europe. These Rupelian amphicyonids, belonging to Amphicyoninae and Haplocyoninae, most likely originated from Priabonian stem amphicyonids and entered Europe through migration events, as Rhinocerotidae and Artiodactyla probably did in the earliest Rupelian (Tissier et al., 2018; Weppe et al., 2023). These new arrivals may have been facilitated by a new land connection with Asia, as the Turgai Strait dried out (Pomerol, 1967) in response to glacio-eustatic sea-level fall (Haq et al., 1987). The hypothesis that some amphicyonids dispersed from Asia into Europe in the earliest Oligocene following prey dispersal is thus not rejected by our results, even though, as far as we know, no amphicyonid has yet been clearly retrieved in the Oligocene of Asia (Peigné et al., 2006).

From MP23 to MP26, European carnivorous faunas are characterized by the absence of amphicyonids. This

disappearance is part of a major diversity decrease that likely affected European mammalian fauna as a whole, being documented in rodents (decrease around MP25-MP26, Vianey-Liaud & Schmid, 2009) and nimravid carnivorans (Peigné, 2000; Rémy et al., 1987; Solé et al., 2022a).

The reappearance of amphicyonids during the Chattian (MP26-29) in Europe might be explained by a putative migration from Asia around MP26 (or later) or an endemic evolution from the Rupelian fauna. The latter hypothesis might be supported by the presence of amphicyonines in the Rupelian, for example *Pseudocyonopsis*; while the former hypothesis might be supported by the first appearance of thaumastocyonines in Europe (late Chattian MP29). A generalized dispersal event across Eurasia around MP28 has been described as the '*Microbunodon* Event', based on hoofed mammals (Mennecart, 2015; Scherler et al., 2013), an event perhaps related to the Alpine orogeny and the Late Oligocene Warming that occurred around 23–26 Ma. Likewise, some amphicyonids may have dispersed during this event, such as thaumastocyonines and the rare amphicyonine *Goupilictis* (first occurrence in MP28; Bonis, 2015).

Our analysis of the Paleogene amphicyonids allows for relating the Chattian amphicyonid fauna with what we know about the early Miocene amphicyonids (Solé et al., 2022b; Viranta, 1996). The structure of the Chattian amphicyonid fauna (*e.g.*, abundance of taxa, large thaumastocyonines, numerous haplocyonines and amphicyonines around 30–50 kg) recalls that of the earliest Miocene (MN1-2; MN = Mammal Neogene reference levels) of Europe (Solé et al., 2022b). This changed after MN3 with the disappearance of Haplocyoninae (Peigné & Heizmann, 2003; Solé et al., 2022b). However, amphicyonid fauna from the earliest Miocene differs in the presence of a bone-crushing mesocarnivore (= scavenger) amphicyonid: *Amphicyon*. This ecomorphotype is indeed unknown in the Oligocene.

As the evolution of the amphicyonids now can be traced back from their appearance (*Cynodictis*; Priabonian, MP18) until their extinction (*Amphicyon pannonicus*; Messinian, MN12) in Europe—a 30 million year history (*ca.* 37–7 Mya)—this compilation of discoveries will be useful to compare the evolution of amphicyonids worldwide, or for comparing their evolutionary dynamics with other carnivorans or their potential prey (e.g. artiodactyls and perissodactyls). It can be used to determine migration phases and/or the possible iterative appearance of ecomorphological adaptations. Here we present some preliminary remarks. The Oligocene amphicyonids of North America include only species belonging to the endemic daphoenines and temnocyonines (Hunt, 2009). The North American amphicyonids from the Paleogene were thus isolated from those of Eurasia. In the Rupelian, no daphoenine attained a large size; they all have a body mass inferior to 25 kg (Hunt, 2009). They were thus possibly ecologically similar to the Priabonian *Cynodictis* of Europe. Conversely, we find amphicyonids of 50 kg in the Rupelian of Europe (see above). The Chattian of North America is characterized by the appearance of large hypercarnivores (up to 40–100 kg) and bone-crushing mesocarnivore belonging to temnocyonines (Hunt, 2009, 2011). Thaumastocyoninae and Amphicyoninae only arrived in North America during the early Miocene while they are known since the Oligocene in Europe (see above). In North America, they are then represented by the genera *Ysengrinia*, *Cynelos*, and *Amphicyon* (Hunt, 2002, 2003; Hunt & Stepleton, 2015; Hunt & Yatkola, 2020). The appearance of *Cynelos* and *Amphicyon* are hypothesized to have been partially associated with the extinction of Temnocyoninae (Hunt, 2011).

Amphicyonidae arrived in Africa only during the Miocene (*ca.* 19–5.5 Mya) and the amphicyonines were as abundant on that continent as they were in Europe (Morales et al., 2016; Werdelin & Peigné, 2010). Moreover, the African amphicyonines *Hecubides*, *Afrocyon*, and *Myacyon* may represent endemic clades (Morales et al., 2016). In Asia, nearly all known amphicyonids are amphicyonines (Peigné et al., 2006); numerous species being referred to *Amphicyon* (Peigné et al., 2006) or closely related to this taxon (*e.g.*, *Arctamphicyon*—Sun et al., 2022). Only one occurrence of *Ysengrinia* in Asia is reported (in Japan—Kohno, 1997). It is undeniable that Amphicyoninae and, to a lesser extent, Thaumastocyoninae were clearly able to disseminate worldwide and were successful in doing so. However, their relationships with the earliest amphicyonids such as *Gustafsonia* and *Cynodictis* remain to be determined to better understand this evolutionary success.

Conclusions

Carnivora is an emblematic clade in the mammalian fossil record. They have represented the main clade of predatory mammals for the last 30 million years. Yet their origins remain paleontologically poorly recorded. To address this issue, one of their first representatives, the Amphicyonidae, are a key clade, and among them, especially their oldest representatives. Here we provide an extensive comparative description of the cranium of the first European representative, *Cynodictis lacustris*, coupled with several biological interpretations and paleoecological inferences for European Paleogene amphicyonids. We interpret *Cynodictis* as a highly abundant fox-like carnivore in Western Europe, having potentially survived the '*Grande Coupure*'. The diversification of amphicyonids in Europe followed a complex pattern connected to

the Asian continent. The present contribution underlines the crucial importance of studying the Asian fossil record in greater depth now that the earliest North American and European representatives are better known. A global review of Amphicyonidae is becoming increasingly essential for understanding the history of the Caniformia, both in terms of taxonomy and overall systematics, as well as their complex palaeoecological history over 30 million years, or more, during which they have roamed the earth until their unexplained extinction.

Supplementary Information

The online version contains supplementary material available at https://doi.org/10.1186/s13358-025-00350-z.

Supplementary material 1: Table S1. Additional Paleoecological data for Table 3. Symbol: ?, missing data; -, not computed. *BL* Blade length, *BSP* Bayerische Staatssammlung für Paläontologie und historische Geologie, Munich, *m1* lower first molar, *m1L* lower first molar length, *MHNB* Muséum d'Histoire Naturelle de Bâle, *NHMV* Natural History Museum of Vienna, *PMW* PreMolar Width, *RBL* Relative Blade Length, *RPS* Relative Premolar Size.

Acknowledgements
We would like to warmly thank our late colleague Stéphane Peigné (MNHN) for his crucial help in setting up the present project. We thank Christian de Muizon (MNHN) for his help in selecting the specimen for study with S.L. We thank the collection managers, Christine Argot (MNHN), Guillaume Billet (MNHN), and Lionel Cavin (MHNG) for loaning the specimens. We would also like to thank Claire Sagne (MNHN) for access to the MNHN collections. For the photographs of the Paris specimens, we warmly thank Lilian Caze (MNHN) and Philippe Loubry (MNHN). For photos of comparative specimens, we would like to thank Emmanuelle ROBERT, Curator of the Geology Collections at the University of Lyon, Didier BERTHET, from the Musée des Confluences Conservation Center, and Stéphane DUCROCQ, CNRS Research Director at the institut de Paléontologie Humaine: Evolution et Paléoenvironnements (iPHEP). We would like to thank Louis de Bonis (University of Poitiers) for discussions concerning the central specimen of the study and the case of *Cynodictis*. Finally, we would also like to thank the anonymous reviewers and the editors for their assessment, which helped us improve the present manuscript.

Author contributions
Conceptualization: S.L., F.S.; Methodology: K.L.V., S.L., F.S.; Investigation: K.L.V., S.L., F.S.; Visualization: K.L.V., C.L., S.L., F.S.; Drawings: C.L.; Funding Support: S.L., F.S., M.R.S.V.; Supervision: S.L., F.S., V.F., M.R.S.V.; Writing – original draft: K.L.V., F.S.; Writing – review & editing: K.L.V., S.L., C.L., V.F., M.R.S.V., F.S. The last two authors, S.L. and F.S., have contributed equally to the present work.

Funding
The present study is part of the ENLIVEN project of the French National Research Agency (ANR-22-CE02-0014-01) coordinated by Maeva Orliac (University of Montpellier, ISEM) and was also supported by the BELSPO projects Brain Pioneer BR/175/PI/CarnAges of the Belgian Federal Science Policy Office.

Availability of data and materials
No datasets were generated or analysed during the current study.

Declarations

Competing interests
The authors declare no competing interests.

Received: 20 May 2024 Accepted: 23 January 2025
Published online: 19 March 2025

References

Astruc, J. G., Escarguel, G., Maranda, B., Simon-Coinçon, R., & Sigé, B. (2000). Floor-age constraining of a tectonic paroxysm of the pyrenean orogeny. Late middle eocene mammal age of a faulted karstic filling of the quercy phosphorites, south-western France. *Geodinamica Acta, 13*(5), 271–280.

Bastl, K., Nagel, D., & Peigné, S. (2014). Milk tooth morphology of small-sized *Hyaenodon* (Hyaenodontidae, Mammalia) from the European Oligocene–evidence of a *Hyaenodon* lineage in Europe. *Palaeontographica Abteilung A, 303*(1–3), 61–84.

Biknevicius, A. R., Van Valkenburgh, B., & Walker, J. (1996). Incisor size and shape: Implications for feeding behaviors in saber-toothed "cats." *Journal of Vertebrate Paleontology, 16*(3), 510–521.

Biochrom, M. (1997). Tableaux de corrélations et synthèses. Actes du Congrès BiochroM'97. *Mémoires Et Travaux De L'institut De Montpellier De L'ecole Pratique Hautes Etudes, 21*, 769–805.

Bowdich, T. E. (1821). *An analysis of the natural classification of mammals for the use of students and travellers* (p. 115). J. Smith.

Bravard, A., & Pomel, A. (1850). *Notice sur les ossements fossiles de la Débruge* (p. 8). J.-S. Jean.

Carlsson, A. (1914). On the fossil Carnivores *Cynodictis intermedius* and *Cynodon gracilis* from the phosphorites of quercy. *Proceedings of the Zoological Society of London, 84*(2), 227–230. https://doi.org/10.1111/j.1469-7998.1914.tb07031.x

Cavaillé, A. (1974). La région des phosphorites du quercy. *Palaeovertebrata, 6*, 5–19.

Chow, M., Li, C.-K., & Chang, Y. (1973). Late Eocene mammalian faunas of Honan and Shansi with notes on some vertebrate fossils collected therefrom. *Vertebrata PalAsiatica., 11*, 166–181.

Costa, E., Garcés, M., Sáez, A., Cabrera, L., & López-Blanco, M. (2011). The age of the "Grande Coupure" mammal turnover: New constraints from the eocene-oligocene record of the Eastern Ebro Basin (NE Spain). *Palaeogeography, Palaeoclimatology, Palaeoecology, 301*(1–4), 97–107.

David, A. (1869). Extrait d'une lettre du mem, datée de la principauté thibétaine (indépendante) de Mou-pin, le 21 Mars 1869. *Nouvelles Archives Du Muséum D'histoire Naturelle, 5*, 12–13.

de Bonis, L. (1966). Sur l'évolution du genre *Haplocyon* Schlosser (Carnivora). *Bulletin De La Société Géologique De France, 8*, 114–117. https://doi.org/10.2113/gssgfbull.S7-VIII.1.114

de Bonis, L. (1978). La poche à phosphate de Ste-Neboule (Lot) et sa faune de vertébrés du Ludien supérieur. 12.—Fissipèdes (Carnivores). *Palaeovertebrata, 8*, 301–311.

de Bonis, L. (2015). Revival of a species of the rare European Oligocene amphicyonid *Goupilictis* Ginsburg, 1969 (Mammalia, Carnivora, Amphicyonidae). *Journal of Vertebrate Paleontology, 35*(5), e969401.

de Bonis, L. (2020). New genus of amphicyonid carnivoran (Mammalia, Carnivora, Amphicyonidae) from the phosphorites of Quercy (France). *Fossil Imprint, 76*(1), 201–208.

de Bonis, L., Crochet, J. Y., Rage, J. C., Sigé, B., Sudre, J., & Vianey-Liaud, M. (1973). Nouvelles faunes de Vertébrés oligocènes des phosphorites du quercy. *Bulletin Du Muséum National D'histoire Naturelle, 28*, 105–113.

de Bonis, L., Gardin, A., & Blondel, C. (2019). Carnivora from the early oligocene of the 'phosphorites du quercy' in southwestern France. *Geodiversitas, 41*(15), 601–621.

Teilhard de Chardin, P. (1915). Les carnassiers des phosphorites du quercy. *Annales De Paléontologie, 9*, 101–192.

Dehm, R. (1935). Über tertiäre Spaltenfüllungen im Fränkischen und Schwäbischen Jura. *Abhandlungen der bayerischen Akademie der Wissenschaften, Mathematisch-Naturwissenschaftliche Abteilung. Neue Folge, 29*, 1–86.

Dombrowski, M. (1888). Mes chasses aux fossiles dans le Lot-et-Garonne (Souvenir géologique). *Journal D'histoire Naturelle De Bordeaux Et Du Sud-Ouest, 9*, 97–99.

Egi, N., Tsubamoto, T., & Tsogtbaatar, K. (2009). New amphicyonid (Mammalia: Carnivora) from the upper eocene ergilin dzo formation, Mongolia. *Paleontological Research, 13*, 245–249. https://doi.org/10.2517/1342-8144-13.3.245

Escarguel, G., Legendre, S., & Sigé, B. (2008). Unearthing deep-time biodiversity changes: The palaeogene mammalian metacommunity of the quercy and Limagne area (Massif Central, France). *Comptes Rendus Geoscience, 340*(9–10), 602–614.
Evans, H. (1993). *Miller's anatomy of the dog* (p. 1113). W.B. Saunders Company.
Filhol, H. (1876). Recherches sur les phosphorites du Quercy. Études des fossiles qu'on y rencontre et spécialement des mammifères. *Bibliothèque de l'École des Hautes Études, Section des Sciences naturelles. Première partie*, *15*(4), 1–220.
Filhol, H. (1872). Recherches sur les mammifères fossiles des dépôts de phosphate de chaux dans les départements du Lot, du Tarn, et de Tarn-et-Garonne. Première partie: carnassiers et chiroptères. *Annales des Sciences Géologiques, 3*(7), 1–31.
Filhol, H. (1874). Sur les Vertébrés fossiles des dépôts de phosphate de chaux du quercy. *Bulletin De La Société Philomatique De Paris, 11*, 16–20.
Filhol, H. (1879). Étude des mammifères fossiles de saint-gérand-le-puy (Allier). *Annales des Sciences Géologiques, 10*, 1–252.
Filhol, H. (1880). Sur la decouverte de mammiferes nouveaux dans les depots de phosphates de chaux du Quercy. *Comptes Rendus De L'académie des Sciences, 90*, 1579–1580.
Filhol, H. (1882). *Mémoires sur quelques mammifères fossiles des phosphorites du quercy* (p. 180). Vialelle et cie. https://doi.org/10.5962/bhl.title.86309
Finarelli, J. A. (2008). A total evidence phylogeny of the Arctoidea (Carnivora: Mammalia): Relationships among basal taxa. *Journal of Mammalian Evolution, 15*, 231–259. https://doi.org/10.1007/s10914-008-9074-x
Flynn, J. J., Finarelli, J. A., & Spaulding, M. (2010). Phylogeny of the Carnivora and Carnivoramorpha, and the use of the fossil record to enhance understanding of evolutionary transformations. *Carnivoran evolution*, 25–63.
Gervais, P. (1852). *Zoologie et paléontologie françaises: Nouvelles recherches sur les animaux vertébrés dont on trouve les ossements enfouis dans le sol de la France*. Arthus Bertrand. https://doi.org/10.5962/bhl.title.39473
Gèze, B. (1974). Sur le remplissage des poches à phosphorite d'aubrelong (Commune de Bach, Lot). *Palaeovertebrata, 6*, 21–25.
Ginsburg, L. (1965). L'"*Amphicyon" ambiguus* des phosphorites du quercy. *Bulletin Du Muséum National D'histoire Naturelle, 37*(4), 724–730.
Ginsburg, L. (1966). Les amphicyons des phosphorites du quercy. *Annales De Paléontologie, 52*, 23–64.
Ginsburg, L. (1999). Order Carnivora. In G. E. Rössner & K. Heissig (Eds.), *The miocene land mammals of Europe* (pp. 109–148). Munich.
Goswami, A., & Friscia, A. (2010). *Carnivoran evolution: new views on phylogeny, form and function* (p. 506). Cambridge University Press.
Gray, J. E. (1830). *Spicilegia zoologica; or original figures and short systematic descriptions of new and unfigured animals* (p. 12). Treutel, Würtz and Co., and W. Wood.
Haq, B. U., Hardenbol, J. A. N., & Vail, P. R. (1987). Chronology of fluctuating sea levels since the Triassic. *Science, 235*(4793), 1156–1167.
Helbing, H. (1928). Carnivoren des oberen stampien. *Abhandlungen der Schweizerischen Palaeontologischen Gesellschaft, 47*, 1–82.
Hough, J. R. (1948). A systematic revision of *Daphoenus* and some allied genera. *Journal of Paleontology, 22*, 573–600.
Hunt, R. M. (1977). Basicranial anatomy of *Cynelos* Jourdan (Mammalia: Carnivora), an aquitanian amphicyonid from the Allier Basin, France. *Journal of Paleontology, 51*, 826–843.
Hunt, R. M. (1996). Amphicyonidae. The terrestrial eocene-oligocene transition in North America. In D. R. Prothero & W. A. Berggren (Eds.), *Eocene-oligocene climatic and biotic evolution* (pp. 476–485). Cambridge University Press.
Hunt, R. M., Jr. (1998). Amphicyonidae. In C. M. Janis, K. M. Scott, & L. L. Jacob (Eds.), *Evolution of tertiary mammals of North America* (pp. 196–227). Cambridge.
Hunt, R. M., Jr. (2002). Intercontinental migration of Neogene amphicyonids (Mammalia, Carnivora): Appearance of the eurasian beardog *Ysengrinia* in North America. *American Museum Novitates, 3384*, 1–53.
Hunt, R. M., Jr. (2003). Intercontinental migration of large mammalian carnivores: Earliest occurrence of the old world beardog *Amphicyon* (Carnivora, Amphicyonidae) in North America. *Bulletin of the American Museum of Natural History, 279*, 77–115.
Hunt, R. M., Jr. (2009). Long-legged pursuit carnivorans (Amphicyonidae, Daphoeninae) from the early Miocene of North America. *Bulletin of the American Museum of Natural History, 2009*(318), 1–95.
Hunt, R. M., Jr. (2011). Evolution of large carnivores during the mid-cenozoic of North America: The temnocyonine radiation (Mammalia, Amphicyonidae). *Bulletin of the American Museum of Natural History, 2011*(358), 1–153.
Hunt, R. M., Jr., & Stepleton, E. (2015). A skull of the immigrant eurasian beardog *Cynelos* (Carnivora, Amphicyonidae) from the early miocene of southern California. *Journal of Vertebrate Paleontology, 35*(1), e891229.
Hunt, R. M., Jr., & Yatkola, D. A. (2020). A new species of the amphicyonid carnivore *Cynelos* Jourdan, 1862 from the early Miocene of North America. *Geodiversitas, 42*(5), 57–67.
Kohno, N. (1997). The first record of an amphicyonid (Mammalia: Carnivora) from Japan, and its implication for amphicyonid paleobiogeography. *Paleontological Research, 1*(4), 311–315.
Kotsakis, T. (1980). Revisione sistematica e distribuzione stratigrafica e geografica del genere *Cynodictis* Bravard & Pomel (Carnivora, Mammalia). *Bollettino della Società Paleontologica Italiana, 19*, 259–273.
Lange-Badré, B. (1979). Les Créodontes (Mammalia) d'Europe occidentale de l'Éocène supérieur à l'Oligocène supérieur. *Mémoires du Muséum national d'Histoire naturelle – Sciences de la Terre*, *42*, 1–249.
Le Verger, K., Solé, F., & Ladevèze, S. (2020). Description of a new species of *Cynodictis* Bravard & Pomel, 1850 (Carnivora, Mammalia) from the quercy phosphorites with comments on the use of skull morphology for phylogenetics. *Geodiversitas, 42*(16), 239–255. https://doi.org/10.5252/geodiversitas2020v42a16
Legendre, S. (1987). Les communautés de mammifères d'Europe occidentale de l'Eocène supérieur et Oligocène: Structures et milieux. *Münchner Geowissenschaftliche Abhandlungen (a), 10*, 301–312.
Legendre, S., Crochet, J. Y., Godinot, M., Hartenberger, J. L., Marandat, B., Remy, J. A., Sigé, B., Sudre, J., & Vianey-Liaud, M. (1991). Evolution de la diversité des faunes de mammifères d'Europe occidentale au Paléogène (MP 11 à MP 30). *Bulletin De La Société Géologique De France, 162*, 867–874.
Legendre, S., & Hartenberger, J. L. (1992). Evolution of Mammalian faunas in Europe during the eocene and oligocene. In D. R. Prothero & W. A. Berggren (Eds.), *Eocene—oligocene climatic and biotic evolution* (pp. 516–528). Princeton.
Legendre, S., Marandat, B., Sigé, B., Crochet, J. Y., Godinot, M., Hartenberger, J. L., Sudre, J., Vianey-Liaud, M., Muratet, B., & Astruc, J. G. (1992). Mammalian fauna of vielase (phosphorites of Quercy, in the South of France): Paleontological evidence for karst formation in the quercy area as early as the early eocene. *Neues Jahrbuch Für Geologie und Paläontologie-Monatshefte, 1992*, 414–428.
Linnaeus, C. (1758). *Systema naturæ per regna tria naturæ, secundum classes, ordines, genera, species, cum characteribus, differentiis, synonymis, locis* (pp. 824). Volume 1. Salvius, Holmiæ. https://doi.org/10.5962/bhl.title.559
Macphee, R. D. E. (1981). Auditory regions of primates and eutherian insectivores. *Contributions to Primatology, 18*, 1–282.
Maitre, E., Hugueney, M., Astruc, J.-G., Crochet, J.-Y., Escarguel, G., Godinot, M., Legendre, S., Marandat, B., Mourer-Chauviré, C., Rage, J.-C., Remy, J. A., Simon-Coinçon, R., Sudre, J., Valette, P., & Sigé, B. (2006). Huit nouvelles faunes éocènes et oligocènes des Phosphorites du Quercy. In 'Strata' (Ed.), *30 millions d'années de biodiversité dynamique dans le paléokarst du Quercy*, *13*, 113–127.
Maitre, E. (2014). Western European middle eocene to early oligocene chiroptera: Systematics, phylogeny and palaeoecology based on new material from the Quercy (France). *Swiss Journal of Palaeontology, 133*(2), 141–242.
Maitre, E., Sigé, B., & Escarguel, G. (2008). A new family of bats in the paleogene of Europe: Systematics and implications for the origin of emballonurids and rhinolophoids. *Neues Jahrbuch fur Geologie und Palaontologie-Abhandlungen, 250*(2), 1–199.
Mathis, C. (1985). Contribution à la connaissance des mammifères de Robiac (Éocène supérieur): Creodonta et Carnivora. *Bulletin Du Muséum National D'histoire Naturelle, Section C, 7*(4), 305–326.
Matthew, W. D., & Granger, W. (1924). New Carnivora from the Tertiary of Mongolia. *American Museum Novitates, 104*, 1–9.
McKenna, M. C., & Bell, S. K. (1997). *Classification of mammals: above the species level* (p. 640). Columbia University Press.

Mennecart, B. (2015). The European ruminants during the "Microbunodon Event"(MP28, latest Oligocene): Impact of climate changes and faunal event on the ruminant evolution. *PLoS ONE, 10*(2), e0116830.
Morales, J., Pickford, M., & Valenciano, A. (2016). Systematics of African Amphicyonidae, with descriptions of new material from Napak (Uganda) and Grillental (Namibia). *Journal of Iberian Geology, 42*(2), 131–150.
Noulet, J. B. (1876). Note sur un gisement du *Canis palaeolycos*, dans le Miocene toulousain. *Mémoires De L'académie des Sciences, Inscriptions Et Belles-Lettres De Toulouse, 8*, 400–403.
Pallas PS (1780). Spicilegia Zoologica, quibus novae imprimis et obcurae animalium species iconibus (Berolini, G. A. Lange, 1774–1780. Fasicle 14, p. 5). *Catalogue of the Library of the Museum of Comparative Zoology*, *6:* 506.
Peigné, S. (2000). A new species of *Eofelis* (Carnivora: Nimravidae) from the phosphorites of quercy, France. *Comptes Rendus De L'académie des Sciences-Series IIA-Earth and Planetary Science, 330*(9), 653–658.
Peigné, S., Chaimanee, Y., Yamee, C., Tian, P., & Jaeger, J. J. (2006). A new amphicyonid (Mammalia, Carnivora, Amphicyonidae) from the late middle Miocene of northern Thailand and a review of the amphicyonine record in Asia. *Journal of Asian Earth Sciences, 26*(5), 519–532.
Peigné, S., & Heizmann, E. P. J. (2003). The Amphicyonidae (Mammalia: Carnivora) from Ulm-Westtangente (MN 2, Early Miocene), baden-württemberg, Germany—systematics and ecomorphology. *Stuttgarter Beiträge Zur Naturkunde Serie B (Geologie und Paläontologie), 343*, 1–133.
Peigné, S., Vianey-Liaud, M., Pélissié, T., & Sigé, B. (2014). Valbro: Un nouveau site à vertébrés de l'Oligocène inférieur (MP22) de France (Quercy). I—contexte géologique; Mammalia: Rodentia, hyaenodontida Carnivora. *Annales De Paléontologie, 100*, 1–45. https://doi.org/10.1016/j.annpal.2013.11.002
Petter, G. (1966). *Cynodictis*: Canidé oligocène d'Europe, région tympanique et affinités. *Annales De Paléontologie, 52*, 1–19.
Pomel, A. (1846). Mémoire pour servir à la géologie paléontologique des terrains tertiaires du département de l'Allier. *Bulletin De La Société Géologique De France, 3*, 353–373.
Pomerol, C. (1967). Esquisse paléogéographique du Bassin de Paris, à l'ère tertiaire et aux temps quaternaires. *Revue De Géographie Physique Et De Géolologie Dynamique, 9*, 35–85.
Reighard, J., & Jennings, H. S. (1935). *Anatomy of the cat* (3rd ed., p. 486). Henry Holt and Company.
Remy, J. A., Crochet, J. Y., Sioe, B., Sudre, J., de Bonis, L., Vianey-Liaud, M., Godinot, M., Hartenberger, J. L., Lange-Badré, B., & Comte, B. (1987). Biochronologie des phosphorites du quercy : Mise à jour des listes fauniques et nouveaux gisements de mammifères fossiles. *Münchner Geowissenschaftliche Abhandlungen (a), 10*, 169–188.
Renault, P., Guillot, P. L., Lefavrais-Raymond, A., Seronie-Vivien, M. R., Cavaillé, A., & Clottes, J. (1978). Géologie du quercy. *Les Suppléments De Quercy Recherche, Série Études Et Travaux, 4*, 1–111.
Rose, K. D. (2006). *The beginning of the age of mammals* (p. 428). John Hopkins University Press.
Russell, D. E., & Zhai, R.-J. (1987). The paleogene of Asia: Mammals and stratigraphy. *Mémoires Du Muséum National D'histoire Naturelle Série C Sciences De La Terre, 52*, 1–488.
Scherler, L., Mennecart, B., Hiard, F., & Becker, D. (2013). Evolution of terrestrial hoofed-mammals during the oligocene-miocene transition in Europe. *Swiss Journal of Geosciences, 106*, 349–369.
Schlosser, M. (1887). Die affen, lemuren, chiropteren, insectivoren, marsupialier, creodonten und Carnivoren des europaischen tertiärs und deren beziehungen zu ihren lebenden und fossilen aussereuropdischen verwandten I-II. *Beiträge Zur Paläontologie Österreich-Ungarns und des Orient, 6*, 1–227.
Schlosser, M. (1899). Über die Bären und bärenähnlichen Formen des europäischen Tertiärs. *Palaeontographica, A, 46*, 95–148.
Shaw G, Nodder, FP (1791). The Ursine *Bradypus,* or Ursiform Sloth. *The Naturalists Miscellany.* 2: 58–59.
Sigé, B., Aguilar, J. P., Marandat, B., & Astruc, J. G. (1991). Extension au Miocène inférieur des remplissages phosphatés du Quercy. La faune de vertébrés de Crémat (Lot, France). *Geobios, 24*(4), 497–502.
Solé, F., Fischer, V., Denayer, J., Speijer, R. P., Fournier, M., Le Verger, K., Ladevèze, S., Folie, A., & Smith, T. (2021). The upper eocene-oligocene carnivorous mammals from the quercy phosphorites (France) housed in Belgian collections. *Geologica Belgica, 24*(1–2), 1–16.
Solé, F., Fischer, V., Le Verger, K., Mennecart, B., Speijer, R. P., Peigné, S., & Smith, T. (2022a). Evolution of European carnivorous mammal assemblages through the Palaeogene. *Biological Journal of the Linnean Society, 135*(4), 734–753.
Solé, F., Gheerbrant, E., & Godinot, M. (2011). New data on the oxyaenidae from the early eocene of Europe; biostratigraphic, paleobiogeographic and paleoecologic implications. *Palaeontologia Electronica, 14*, 13–41.
Solé, F., Lesport, J. F., Heitz, A., & Mennecart, B. (2022b). A new gigantic carnivore (Carnivora, Amphicyonidae) from the late middle Miocene of France. *PeerJ, 10*, e13457.
Solé, F., Smith, R., Coillot, T., de Bast, E., & Smith, T. (2014). Dental and tarsal anatomy of '*Miacis*' *latouri* and a phylogenetic analysis of the earliest carnivoraforms (Mammalia, Carnivoramorpha). *Journal of Vertebrate Paleontology, 34*, 1–21.
Solé, F., Smith, T., de Bast, E., Codrea, V., & Gheerbrant, E. (2016). New carnivoraforms from the latest paleocene of Europe and their bearing on the origin and radiation of carnivoraformes (Carnivoramorpha Mammalia). *Journal of Vertebrate Paleontology*. https://doi.org/10.1080/02724634.2016.1082480
Spaulding, M., & Flynn, J. J. (2012). Phylogeny of the Carnivoramorpha: The impact of postcranial characters. *Journal of Systematic Palaeontology, 10*, 653–677. https://doi.org/10.1080/14772019.2011.630681
Springhorn, R. (1977). Revision der alttertiären europäischen Amphicyonidae (Carnivora, Mammalia). *Palaeontographica Abteilung A, 158*(1–3), 26–113.
Stehlin, H. G. (1909). Remarques sur les faunules de mammifères des couches éocènes et oligocènes du Bassin de Paris. *Bulletin De La Société Géologique De France, 9*, 488–520.
Sun, Z., Han, A., Li, Y., Jiangzuo, Q., Wang, S., & Li, S. (2022). New material of *Amphicyon zhanxiangi* from laogou, linxia basin suggests a possible southern dispersal with increasing omnivory. *Historical Biology, 34*(5), 857–864.
Szalay, F. S. (1969). Mixodectidae, microsyopidae, and the insectivore-primate transition. *American Museum of Natural History Bulletin, 140*, 193–330.
Tissier, J., Becker, D., Codrea, V., Costeur, L., Fărcaş, C., Solomon, A., Venczel, M., & Maridet, O. (2018). New data on amynodontidae (Mammalia, Perissodactyla) from Eastern Europe: Phylogenetic and palaeobiogeographic implications around the Eocene-Oligocene transition. *PLoS ONE, 13*(4), e0193774.
Tomiya, S. (2011). A new basal caniform (Mammalia: Carnivora) from the middle Eocene of North America and remarks on the phylogeny of early carnivorans. *PLoS ONE, 6*(9), e24146. https://doi.org/10.1371/journal.pone.0024146
Tomiya, S., & Tseng, Z. J. (2016). Whence the beardogs? Reappraisal of the Middle to Late Eocene '*Miacis*' from Texas, USA, and the origin of Amphicyonidae (Mammalia, Carnivora). *Proceedings of the Royal Society, 3*, 160518. https://doi.org/10.1098/rsos.160518
Tomiya, S., Zack, S. P., Spaulding, M., & Flynn, J. J. (2021). Carnivorous mammals from the middle Eocene Washakie Formation, Wyoming, USA, and their diversity trajectory in a post-warming world. *Journal of Paleontology, 95*(S82), 1–115.
Trouessart, E. (1885). Catalogue des mammifères vivants et fossils—Carnivores. *Bulletin De La Société D'études Scientifiques D'angers, 15*, 1–108. https://doi.org/10.5962/bhl.title.63808
Tsubamoto, T., Egi, N., Takai, M., Shigehara, N., Suzuki, H., Nishimura, T., Ugai, H., Maung, M., Chit, S., Soe Thura, T., Naing Soe, A., Ko Aung, A., Thein, T., Thaung, H., & Zin, M. M. T. (2006). A summary of the pondaung fossil expeditions. *Asian Paleoprimatology, 4*, 1–66.
Van Valkenburgh, B. (1988). Trophic diversity in past and present guilds of large predatory mammals. *Paleobiology, 14*, 155–173.
Van Valkenburgh, B. (1990). Skeletal and dental predictors of body mass in carnivores. In J. Damuth & B. J. MacFadden (Eds.), *Body size in Mammalian paleobiology* (pp. 181–206). Cambridge University Press.
Van Valkenburgh, B. (1991). Iterative evolution of hypercarnivory in canids (Mammalia: Carnivora): Evolutionary interactions among sympatric predators. *Paleobiology, 17*(4), 340–362.
Van Valkenburgh, B. (2007). Déjà vu: The evolution of feeding morphologies in the Carnivora. *Integrative and Comparative Biology, 47*, 147–163.
Vianey-Liaud, M., & Schmid, B. (2009). Diversité, datation et paléoenvironnement de la faune de mammifères oligocène de Cavalé (Quercy, SO

France): Contribution de l'analyse morphométrique des theridomyinae (Mammalia, Rodentia). *Geodiversitas, 31*(4), 909–941.
Viranta, S. (1996). European miocene amphicyonidae—taxonomy, systematics and ecology. *Acta Zoologica Fenica, 204*, 1–61.
Viret, J. (1929). Les faunes de mammiferes de l'Oligocene supérieur de la Limagne bourbonnaise. *Annales De L'université De Lyon, Nouvelle Série, 1*(47), 1–329.
von Meyer, H. (1849). Letter on various fossils. *Neues Jahrbuch Für Geologie und Paläontologie, 1849*, 547–550.
Wang, X., Emry, R. J., Boyd, C. A., Person, J. J., White, S. C., & Tedford, R. H. (2022). An exquisitely preserved skeleton of Eoarctos vorax (nov. gen. et. Sp.) from fitterer ranch, North Dakota (early Oligocene) and systematics and phylogeny of North American early arctoids (Carnivora, Caniformia). *Journal of Vertebrate Paleontology, 42*(1), 1–123. https://doi.org/10.1080/02724634.2022.2145900
Weppe, R., Condamine, F. L., Guinot, G., Maugoust, J., & Orliac, M. J. (2023). Drivers of the artiodactyl turnover in insular western Europe at the eocene-oligocene transition. *Proceedings of the National Academy of Sciences, 120*(52), e2309945120.
Werdelin, L., & Peigné, S. (2010). Carnivora. In L. Werdelin & W. J. Sanders (Eds.), *Cenozoic mammals of Africa* (pp. 609–663). Berkeley.
Wesley-Hunt, G. D., & Flynn, J. J. (2005). Phylogeny of the Carnivora: Basal relationships among the Carnivoramorphans, and assessment of the Position of 'Miacoidea' Relative to Carnivora. *Journal of Systematic Palaeontology, 3*, 1–28. https://doi.org/10.1017/S1477201904001518
Wible, J. R., & Spaulding, M. (2013). On the cranial osteology of the african palm civet, *Nandinia binotata* (Gray, 1830) (Mammalia, Carnivora, Feliformia). *Annals of Carnegie Museum, 82*, 1–114. https://doi.org/10.2992/007.082.0101
Wyss, A. R., & Flynn, J. J. (1993). A phylogenetic analysis and definition of the Carnivora. In F. S. Szalay, M. J. Novacek, & M. C. McKenna (Eds.), *Mammal phylogeny—placentals* (pp. 32–52). New York.
Zachos, J., Pagani, M., Sloan, L., Thomas, E., & Billups, K. (2001). Trends, rhythms, and aberrations in global climate 65 Ma to present. *Science, 292*(5517), 686–693.
Zhai, R., Ciochon, R. L., Tong, Y., Savage, D. E., Morlo, M., Holroyd, P. A., & Gunnell, G. F. (2003). An aberrant amphicyonid mammal from the latest Eocene of the Bose Basin, Guangxi, China. *Acta Palaeontologica Polonica, 48*, 293–300.
Zhang, X. Y., Bai, B., & Wang, Y. Q. (2023). Bear or bear-dog? An enigmatic arctoid carnivoran from the late Eocene of Asia. *Frontiers in Earth Science, 11*, 1137891.

Publisher's Note